

1 **Large-scale glacetectonic deformation in response to active ice sheet** 2 **retreat across Dogger Bank (southern central North Sea) during the** 3 **Last Glacial Maximum**

4
5 Emrys Phillips^{1*}, Carol Cotterill¹, Kirstin Johnson¹, Kirstin Crombie¹, Leo James², Simon Carr³ and
6 Astrid Ruiten^{1,3}

7 1 - British Geological Survey, The Lyell Centre, Heriot-Watt University, Research Avenue South, Riccarton, Edinburgh, EH14
8 4AS, Scotland, UK (erp@bgs.ac.uk)

9 2 - RPS Energy Ltd, Goldvale House, 27-41 Church Street West, Woking, Surrey, GU21 6DH, UK

10 3 - Department of Geography, Queen Mary University of London, Mile End Road, London, E1 4NS, UK

11 *corresponding author: erp@bgs.ac.uk

12 **Abstract**

13 High resolution seismic data from the Dogger Bank in the central southern North Sea has revealed
14 that the Dogger Bank Formation records a complex history of sedimentation and
15 penecontemporaneous, large-scale, ice-marginal to proglacial glacetectonic deformation. These
16 processes led to the development of a large thrust-block moraine complex which is buried beneath a
17 thin sequence of Holocene sediments. This buried glacetectonic landsystem comprises a series of
18 elongate, arcuate moraine ridges (200 m up to > 15 km across; over 40-50 km long) separated by
19 low-lying ice marginal to proglacial sedimentary basins and/or meltwater channels, preserving the
20 shape of the margin of this former ice sheet. The moraines are composed of highly deformed (folded
21 and thrust) Dogger Bank Formation with the lower boundary of the deformed sequence (up to 40-50
22 m thick) being marked by a laterally extensive décollement. The ice-distal parts of the thrust
23 moraine complex are interpreted as a "forward" propagating imbricate thrust stack developed in
24 response to S/SE-directed ice-push. The more complex folding and thrusting within the more ice-
25 proximal parts of the thrust-block moraines record the accretion of thrust slices of highly deformed
26 sediment as the ice repeatedly reoccupied this ice marginal position. Consequently, the internal
27 structure of the Dogger Bank thrust-moraine complexes can be directly related to ice sheet
28 dynamics, recording the former positions of a highly dynamic, oscillating Weichselian ice sheet
29 margin as it retreated northwards at the end of the Last Glacial Maximum.

30 **Keywords**

31 Large-scale glacitectonics; Dogger Bank; North Sea; Weichselian glaciation

32 **Highlights**

- 33 · Structural architecture of a glacitectonic landsystem, Dogger Bank, North Sea
- 34 · Detailed study using high-resolution 2D seismic data
- 35 · Large-scale glacitectonics at an oscillating margin during surge-related readvance
- 36 · Deformation during Weichselian ice sheet retreat in the southern central North Sea

37

38 **1. Introduction**

39 The North Sea (c. 500 km wide, 50 to 400 m deep) separating the UK from Scandinavia and northern
40 mainland Europe (Figure 1a) has had a long and complex geological history, commencing with rifting
41 during the Jurassic–Early Cretaceous and followed by subsequent thermal cooling and subsidence
42 (Glennie and Underhill, 1998; Zanella and Coward, 2003). Its more recent history has been
43 dominated by the deposition of a locally thick sequence (over 800 m) of Quaternary sediments
44 (Caston, 1977, 1979; Gatliff *et al.*, 1994). This sedimentary record preserves evidence for the
45 advance of several major ice sheets from the surrounding land masses into the North Sea at
46 different stages during the Quaternary. This glacial history has previously been described in terms of
47 three major glacial episodes, the Elsterian (oldest, Marine Isotope Stage [MIS] 12), Saalian (MIS 10–
48 6), and Weichselian (youngest, MIS 5d–2) stage glaciations, separated by warmer interglacial periods
49 (Eisma *et al.*, 1979; Jansen *et al.*, 1979; Caston 1979; Balson and Cameron, 1985; Sejrup *et al.*, 1987,
50 1995, 2000, 2003; Cameron *et al.*, 1987, 1992; Ehlers, 1990; Graham *et al.*, 2007, 2011; Kristensen *et al.*,
51 2007; Bradwell *et al.*, 2008; Stoker *et al.*, 2011; Stewart *et al.*, 2013; Ottesen *et al.*, 2014; Phillips
52 *et al.*, 2017). However, several recent studies (e.g. Beets *et al.*, 2005; Lonergan *et al.*, 2006; Stewart
53 and Lonergan, 2011) have suggested that there may have been many more glacial episodes. An
54 increasing body of geomorphological and sedimentological data is not only providing the key
55 evidence for the existence of these former Pleistocene ice sheets, but is also being used to
56 demonstrate that they extended across the NW European continental shelves (Graham *et al.*, 2007,
57 2010, 2011; Bradwell *et al.*, 2008; Dunlop *et al.*, 2010; Howe *et al.*, 2012). Consequently, the
58 Quaternary of the North Sea is critical to our understanding the evolution of the major northern
59 European palaeo-ice masses, such as the British and Irish (BIIS) and Fennoscandian (FIS) ice sheets.

60 Several models proposed for the Weichselian glaciation within the North Sea (e.g. Boulton
61 and Hagedorn, 2006; Carr *et al.*, 2006; Graham *et al.*, 2007, 2011; Bradwell *et al.*, 2008; Sejrup *et al.*,
62 2009, 2016; Hughes *et al.*, 2016) require the BIIS and FIS to have converged forming a “confluence
63 zone” within the central part of the basin located to the north of, and between Dogger Bank and
64 Denmark. However, the maximum extents of these major ice masses are poorly constrained
65 resulting in a complex, often conflicting pattern of postulated ice limits within the southern North
66 Sea (see Figure 1a) (e.g. Jansen *et al.*, 1979; Catt, 1991; Clark *et al.*, 2004; Carr *et al.*, 2006; Hubbard
67 *et al.*, 2009; Brooks *et al.*, 2009; Sejrup *et al.*, 1987, 2000, 2009, 2016). Importantly, until recently
68 this lack of understanding was further compounded by the fact that very little was known about the
69 Quaternary sediments underlying the Dogger Bank. Consequently, establishing a robust model for
70 the evolution of Dogger Bank is critical to our understanding Weichselian ice sheet dynamics within
71 this part of the North Sea basin.

72 The Dogger Bank is an isolated, approximately NE-SW-trending topographic high (100 km
73 wide, 250 km long) which is mainly located within the UK sector of the North Sea (Figure 1a), but
74 also extends into Dutch and German territorial waters. The earliest reference to the Dogger Bank
75 being glacial in origin was made by Thomas Belt (1874) who stated that “*The ice north was now*
76 *gradually receding, and leaving great banks of moraine rubbish in the old ocean bed, to be ultimately*
77 *levelled by the sea when it long afterwards returned, and which now form the Dogger and other*
78 *great submarine banks*”. Stride (1959) and Veenstra (1965) also argued for Dogger Bank being a
79 moraine suggesting that this shallow area of the North Sea comprised a “*frame work of moraines*
80 *covered by younger Pleistocene sediments*”. Veenstra (1965) went on to suggest that this “*former*
81 *glaciated landscape covered with soft sediments*” “*consists of moraine ridges belonging presumably*
82 *to the Weichsel glaciation, the last Pleistocene glaciation*”. Subsequent work (Balson and Cameron
83 1985; Cameron *et al.*, 1992) suggested that the stratigraphy and structure of the Dogger Bank was a
84 relatively simple “layer-cake” with the upper 60 m of the Quaternary sedimentary sequence being
85 assigned to the Dogger Bank Formation. However, Wingfield (unpublished) suggested in the late
86 1980s to early 1990s that the Dogger Bank had been pushed from the N (see Carr *et al.*, 2006). Laban
87 (1995) suggested that the wavy nature of the reflectors on the seismic data obtained from the
88 Dogger Bank Formation from several locations within the Dutch and British sectors of the Dogger
89 Bank was consistent with deformation resulting from “*ice-pushing from the north-west*”.
90 Furthermore, van der Meer and Laban (1990) presented micromorphological evidence from the
91 Dogger Bank Formation in the Dutch sector of the Dogger Bank had locally been subjected to glacial
92 shear. However, the extent and complexity of the deformation recorded by the Dogger Bank
93 Formation was still essentially unknown.

94 Recently acquired high-resolution geophysical and ground truthing datasets acquired by the
95 Forewind Consortium (Statoil, Statkraft, RWE and SSE) between 2010 and 2014 (see Figure 1b) as
96 part of the site investigation for a major offshore windfarm development revealed that the
97 Quaternary stratigraphy on the Dogger Bank is far from being a simple “layer cake”. Using these
98 high-resolution datasets Cotterill *et al.* (2017a, b) have been able to demonstrate that the evolution
99 of the Dogger Bank during the Quaternary is far more complex than previously thought and can be
100 directly linked to the interplay between climatic variation, sea level changes (both rise and fall) and
101 ice sheet movement. Importantly these data suggest that during the Weichselian glaciation the
102 Dogger Bank was inundated by ice on more than one occasion.

103 This paper uses high-resolution seismic data from the Dogger Bank to reveal a complex
104 history of sedimentation and penecontemporaneous large-scale, ice-marginal to proglacial
105 glaciectonic deformation recorded by the sediments of the Dogger Bank Formation during the
106 Weichselian stage glaciation. A buried glacial landsystem comprising a series of elongate, arcuate
107 ridges (up to 15-20 km across, over 50 km long) separated by low-lying linear basins and/or
108 meltwater channels has been identified, and interpreted as preserving the changing shape of the
109 former Weichselian ice sheet margin as it retreated northward from Dogger Bank. The moraines
110 within this landsystem are composed of highly deformed Dogger Bank Formation sediments with the
111 geometry of the folds and thrusts being consistent with their formation in response to S/SE-directed
112 ice-push. Consequently, the internal structural architecture of the Dogger Bank glaciectonic
113 complexes can be directly related to ice sheet dynamics, recording the former positions of an
114 oscillating ice sheet margin as it retreated northwards at the end of the Last Glacial Maximum.

115

116 **2. Methods**

117 In 2008 the Forewind consortium (then RWE Npower Renewables, SSE, Statoil and Statkraft)
118 undertook a detailed site investigation of the Dogger Bank Zone (DBZ) as part of the Round 3
119 windfarm development within the North Sea instigated by The Crown Estate. The DBZ is located 125
120 to 290 km to the NE of the Yorkshire coast and occurs entirely within the UK sector of the Dogger
121 Bank (Figure 1). It is the largest of the Round 3 zones and covers an area of 8660 km², with water
122 depths ranging from 18 to 63 m Lowest Astronomical Tide (LAT). An initial regional geophysical
123 survey (conducted in 2010) across the entire DBZ (Figure 1b) involved the acquisition of sub-bottom
124 profiles (Sparker and Pinger), magnetometer, sidescan sonar and multibeam datasets with a grid
125 spacing of 2.5 km. In addition, boreholes and Cone Penetration Tests (CPT's) were also acquired. The
126 same methods were then used to obtain high-resolution datasets over three smaller subareas

127 (Tranches A (2010), B (2011/2012) and C (2013); see Figure 1b), with sub-bottom profiles run at 100
128 m inline and 500 to 1000 m crossline spacing, and 100% coverage of multibeam bathymetry and
129 sidescan sonar.

130 Analysis of the sub-bottom seismic profiles has led to the identification of several laterally
131 extensive reflections which could be traced across the DBZ, and a number of laterally discontinuous
132 ones that although not present everywhere, proved important in understanding the evolution of the
133 Dogger Bank (Cotterill *et al.*, 2017b). These key reflections were then gridded, and the resultant
134 “horizon maps” interpreted in terms of sedimentary landsystems (Figure 2; see section 4). In
135 addition, detailed work was undertaken in Tranche A (see Figure 1b) to gain a greater understanding
136 of glacitectonic deformation, formation of desiccation surfaces, and the lateral variability in
137 sedimentary depositional style. A total of 15 seismic profiles (line spacing 300 m to 1500 m apart)
138 from four key areas within Tranche A (Areas A to D on Figure 2) were selected for analysis in order to
139 gain an understanding of the nature and lateral variation in the relative intensity of glacitectonism,
140 and its spatial and temporal relationship(s) to the formation of the buried ice-marginal landsystem
141 and deposition of the Dogger Bank Formation sequence. The profiles all occur approximately
142 orthogonal to the trend of the glacial landforms (see Figure 2) and are therefore aligned parallel to
143 the proposed direction of ice-push responsible for glacitectonic deformation. Consequently the
144 seismic profiles provide a series of structural cross-sections (e.g. Figures 3, 4, 5 and 6) through the
145 landforms providing a complete record of deformation. Large format, high-resolution digital (jpeg)
146 versions of these structural cross-sections are available on request from the authors and are also
147 provided as supplementary publications.

148 Each seismic profile was exported from IHS Kingdom® as high-resolution digital image files
149 (jpegs) and imported into a commercial computer graphics package (CorelDraw version X6/X7 (64
150 bit)). A graphics package was used for the detailed structural analysis as it not only allows individual
151 reflectors in the seismic profiles to be digitised, but also enables the attribution of different line
152 styles to particular geological structures (e.g. bedding, fold axes, thrusts, faults), and colour coding of
153 polygons representing individual seismo/tectonostratigraphical units, and, where applicable, their
154 constituent sedimentary subunits (Figures 3 to 11). These stratigraphical and sedimentary elements
155 were identified on the basis of differences in their acoustic properties on the seismic profiles
156 (Figures 7 to 11; also see Table 1). It must be stressed that the colours used to distinguish between
157 the sedimentary subunits (packages) present within the relatively undeformed part of the Dogger
158 Bank Formation are not intended to infer any direct correlation of these subunits as
159 seismostratigraphic units, but rather used to highlight the geometry of these individual sediment

160 packages. An approximate depth conversion was calculated to aid correlation of the identified
161 structural/sedimentological features and thicknesses of the sedimentary units were obtained using
162 the following velocities: Water Column - 1550 m/s; Holocene sediments - 1600 m/s; Upper Dogger
163 Bank Formation - 1680 m/s; and Lower Dogger Bank Formation - 1750m/s, based on previous
164 velocities gained from glacial sediments in the North Sea by RPS Energy.

165

166 **3. Regional setting and stratigraphy of the Dogger Bank**

167 Regional mapping of the North Sea basin, completed by the late 1980's and early 1990's (BGS 1989,
168 1991; Cameron *et al.*, 1992) demonstrated that the Quaternary sedimentary sequence in the Dogger
169 Bank area can be up to 800 m thick (one of the thickest occurrences in the North Sea) and comprises
170 a mix of glacial, deltaic and shallow marine deposits (Balson and Cameron, 1985; Cameron *et al.*,
171 1992; Gatliff *et al.*, 1994; Cotterill *et al.*, 2017b). Stoker *et al.* (2011) divided the Quaternary
172 succession in the southern North Sea into three major groups: (i) Southern North Sea Deltaic Group
173 (oldest) ranging in age from Lower Pleistocene to Lower Middle Pleistocene; (ii) Dunwich Group
174 comprising a deltaic sequence of Lower Middle Pleistocene age; and (iii) Californian Glacigenic Group
175 (youngest) ranging from Middle Pleistocene to Holocene in age. The Dogger Bank Formation which
176 dominates the upper 60 m of the Quaternary sequence on the Dogger Bank forms an integral part of
177 the Californian Glacigenic Group (table 7 of Stoker *et al.*, 2011) and was, until recently, described as
178 a tabular unit (up to 45 m thick) composed of stratified to well-bedded sediments deposited in
179 proglacial or glaciolacustrine setting (Cameron *et al.*, 1992). Cameron *et al.* (1992) suggested that
180 these sediments formed in an ice-dammed lake environment, or standing body of water trapped
181 along the confluence between the BISS and FIS (also see Valentin, 1955; Veenstra, 1965). However
182 this interpretation relied heavily on the extrapolation of seismic stratigraphies from adjacent areas.
183 Consequently, until recently, very little was known about the exact nature of the sedimentary
184 sequence beneath the Dogger Bank.

185 Cotterill *et al.* (2017b) have begun to address this lack of understanding by utilising high-
186 resolution seismic and borehole data recently acquired during the DBZ windfarm site survey. These
187 authors provided a revised stratigraphic framework for the Dogger Bank, concluding that the upper
188 part of this sequence (the focus of the present study) can be divided into three main units, namely;
189 (i) the Eem Formation and earlier sediments (oldest) (here referred to as the pre-Dogger Bank
190 Formation deposits), (ii) Dogger Bank Formation (c. 40-50 m thick) and (iii) an overlying thin (< 1 m
191 thick) sequence of fine- to medium-grained Holocene sands (youngest) which are locally being
192 reworked by contemporary marine processes. The pre-Dogger Bank Formation deposits comprises a

193 sequence of dense to very dense poorly sorted, silty to fine-grained sands containing interbeds of
194 hard clay and silty fine sand. The presence of shell fragments and organic matter within the sands
195 has been used to suggest that they were deposited in a marine (?nearshore) environment,
196 consistent with their belonging to either the Eem and/or Egmond Ground formations (Cameron *et*
197 *al.*, 1992; Cotterill *et al.*, 2017b).

198 The overlying Dogger Bank Formation is composed of generally stiff to very stiff clays
199 containing multiple sand-rich layers. Based on the geotechnical responses, combined with lateral
200 extent of significant seismic reflections (Table 1), Cotterill *et al.* (2017b) subdivided the formation
201 into three informal tectonostratigraphy subunits (c.f. Cotterill *et al.*, 2017a) here referred to as the
202 “Basal”, “Lower” and “Upper” Dogger Bank (see Figures 3 to 11). The structurally lowest unit, Basal
203 Dogger Bank (BDB; Table 1), forms a series of discrete, laterally discontinuous ridges which occur
204 immediately above the marine sands of the underlying Eem/Egmond Ground formations (see Figures
205 3 to 6). The top of the Basal Dogger Bank is marked by a strong top reflection (see Figures 7 and 11)
206 with available borehole and engineering data (cone penetration tests) indicating that the sediments
207 (sands, silts and clays) within this zone possess a high degree of over-consolidation (Norwegian
208 Geotechnical Institute, unpublished data). The over-consolidated nature of the sediments at the top
209 of the BDB surface has led to this surface being interpreted as a desiccation surface. Furthermore
210 the degree of over-consolidation requires that the surface to be exposed for a prolonged time
211 period. Consequently, this laterally extensive desiccation surface is thought to have formed as a
212 result of its exposure (terrestrial) to prolonged periglacial weathering and alteration (Norwegian
213 Geotechnical Institute, unpublished data). The lower part of the Dogger Bank Formation is
214 dominated by the Lower Dogger Bank (LDB; Table 1) which ranges from < 5 m up to 40 m thick and
215 forms a series of complex “ridge-like” features (Figures 3 to 6). A strong reflection is locally observed
216 marking the top of the Lower Dogger Bank (see Figures 9 and 10) and is once again interpreted as a
217 subaerial exposure surface. The overlying Upper Dogger Bank (UDB; Table 1) is the structurally
218 highest unit within the Dogger Bank Formation and ranges from \leq 5 m to c. 40 m thick (Figures 3 to
219 6). The UDB is often acoustically well-layered (see Figure 7), with the thicker parts of the sequence
220 apparently draping and infilling topographic lows, forming basin-like features located between the
221 “ridges” of LDB sediments (Figures 3 to 6). In Tranche A the LDB and UDB are locally separated by a
222 thin, laterally discontinuous layer of sand and gravel. Although the Dogger Bank Formation is mainly
223 composed of stiff to very stiff clay and silt, the UDB is distinguished from the underlying units by the
224 increased occurrence of sand containing some organics and detrital micas. The LDB and, to a lesser
225 extent, UDB both show evidence of locally intense glacitectonic deformation.

226

227 **4. Buried thrust-moraine complex within the Dogger Bank Formation**

228 The strong reflections marking the desiccation surfaces at the top of the LDB (Cotterill *et al.*, 2017a,
229 b) define a laterally extensive horizon which has been mapped across the DBZ (Figure 2a). This
230 horizon has been gridded to produce a “map” of the top surface of the deformed lower part of the
231 Dogger Bank Formation. The resultant sub-bottom “horizon map” is shown in Figure 2a. The red and
232 yellow colours represent areas where the upper surface of the deformed sequence is located close
233 to sea bed (minimum depth c. 2.5 m). In contrast, the green and blue colours indicate areas where
234 this surface occurs at a much deeper level (maximum depth c. 66 m below sea bed). The resultant
235 pattern of relatively “topographically higher” (i.e. closer to sea bed) areas defines a number of
236 elongate, arcuate features (Figure 2a) which are interpreted as a series of moraines (purple colours
237 on Figure 2b).

238 The horizon map reveals the presence of a buried glacial landscape (Figure 2b) comprising a
239 number of large, roughly E-W-trending moraines (up to 20 km wide, 90-100 km long, 40-50 m high;
240 labelled MC1 to MC4 on Figure 2) buried beneath the UDB and Holocene sedimentary successions
241 (c.f. Cotterill *et al.*, 2017a, b). These moraines are complex and composed of a number of locally
242 intersecting to cross-cutting, arcuate, approximately E-W-trending ridge-like features (individual
243 ridges \leq 3 km wide) consistent with an overall ice movement direction from the N/NW. These
244 moraines are separated by a series of topographically lower areas interpreted as ice-marginal to
245 proglacial sedimentary basins (up to c. 30 km across) and/or meltwater channels (1-5 km wide)
246 (Figure 2b). Analysis of the subsurface seismic profiles show that the moraine ridges are composed
247 of highly deformed BDB and LDB (up to 40-50 m thick), with the intervening basins being occupied
248 by a sequence of relatively undeformed UDB sediments (Figures 3 to 6) (c.f. Cotterill *et al.*, 2017a).
249 The complex nature of the moraines (Figure 2b) is thought to indicate that they represent periods of
250 stillstand and preserve the changing shape of the ice margin.

251 The remainder of this paper describes the internal structure of the moraine complexes as
252 well as the sedimentary architecture of the intervening basins. This detailed analysis is used to
253 construct a model for the structural evolution of the moraine complexes relating their construction
254 to former ice sheet dynamics.

255

256 **5. Structural and sedimentary architecture of the Dogger Bank Formation**

257 The glacial landform map constructed for the top surface of the deformed lower part of the Dogger
258 Bank Formation was used to identify four key areas for further detailed study (Figure 2) in order to
259 gain an understanding of the nature and lateral variation in the relative intensity of glacitectonism:

- 260 · **Area A** (lines 1 to 4; Figures 2 and 3) – a trending NE-SW and located within the central part
261 of the largest and most complex moraine system (MC1 on Figure 2);
- 262 · **Area B** (lines 5 to 8; Figures 2 and 4) – trending NE-SW and located in the northwestern part
263 the same large moraine complex (MC1 on Figure 2a) where the individual moraine-ridges
264 are less apparent and appear to be cut by a system of meltwater channels (Figure 2b);
- 265 · **Area C** (lines 9 to 11; Figures 2 and 5) – trending NW-SE and located at the southeastern end
266 of the moraine complex (MC1 on Figure 2); and
- 267 · **Area D** (lines 12 to 15; Figures 2 and 6) – trending NW-SE and providing a sub-bottom profile
268 through the entire buried glacial landsystem enabling the relationships between the
269 glacitectonic deformation and deposition of the UDB sediments within the intervening
270 sedimentary basins to be established.

271 The seismic profiles all occur approximately orthogonal to the trend of the axes of the moraine
272 ridges (see Figure 2) and provide a series of structural cross-sections (Figures 3 to 6) orientated
273 parallel to the proposed direction of ice-push responsible for glacitectonism. For ease of description
274 the deformed parts of the Dogger Bank Formation sequence have been divided into 8 structural
275 domains (see Figures 3 to 6) which exhibit a similar style and relative intensity of deformation. The
276 characteristics of each of these domains is summarised in Table 2 (after Cotterill *et al.*, 2017a). A
277 detailed description of the structure and sedimentary architecture of the Dogger Bank Formation in
278 the four key areas is provided below.

279 **5.1. Area A**

280 *5.1.1. Structural geology*

281 The deformed lower part of the Dogger Bank Formation (purple colours on Figure 3) within Area A
282 thickens rapidly towards the NE forming a distinct wedge-shaped unit on all the cross-sections
283 (Figure 3). The relative intensity and complexity of deformation increases northwards, consistent
284 with the cross-sections providing a series of transects from the southern margin (Domains 1 and 2;
285 Table 1, Figure 3) into the core (Domains 3, 4 and 5; Table 2, Figures 3, 7, 8 and 9) of this
286 glacitectonic landform (MC1 on Figure 2). Deformation is dominated by a series of locally well-

287 developed, NE-dipping thrusts and associated SW-verging asymmetrical folds (Figures 7, 8 and 9).
288 The sense of offset of the reflectors across the thrusts records a consistent SW-directed sense of
289 displacement. This, coupled with the geometry of the folds within their hanging-walls, supports the
290 conclusion that ice-push responsible for glacitectonism was primarily directed towards the S/SW.

291 Observed changes in the style and relative intensity of glacitectonism from SW to NE across
292 Area A can be illustrated using line 3 (Figures 7, 8 and 9). At the southern end of this seismic profile
293 (Domains 1 and 2) the deformed part of the Dogger Bank Formation is solely represented by the BDB
294 (Figure 7). This unit thickens northwards where it is increasingly deformed by a series of NE-dipping
295 thrusts which clearly offset a band of bright reflectors equated with a prominent desiccation surface
296 at the top of the BDB (Figure 7). This relationship indicates that the periglacial weathering/alteration
297 responsible for the formation of this desiccation surface proposed by Cotterill *et al.* (2017b) pre-
298 dated thrusting and that there was potentially a significant time gap separating the deposition of the
299 basal part of the Dogger Bank Formation and its subsequent glacitectonism. The thrusts become
300 progressively steeper towards the NE where the larger structures have accommodated up to several
301 hundred metres (c. 100-200m) of displacement (Figures 3 and 7). This increased shortening within
302 the BDB led to folding within the hanging-walls of the thrusts. These thrusts also deform the lower
303 part of the structurally overlying UDB indicating that thrusting locally post-dated the deposition of at
304 least the lower parts of this unit. The thickening of the deformed sequence Domain 1 into Domain 2
305 coupled with progressive increase in the relative intensity of deformation towards the NW is
306 consistent with this part of Area A representing the distal parts of a S/SW-propagating thrust-block
307 moraine.

308 The thrusts affecting the BDB and LDB propagate upwards from a major décollement surface
309 located at the base of the Dogger Bank Formation (Figure 3). This subhorizontal to gently N-dipping
310 basal detachment occurs at a deeper structural level within the northern part of Area A. It climbs
311 upwards (c. 10-15 m vertical climb over a horizontal distance of approximately 2 to 3 km) towards
312 the SW via a number of step-like ramps located beneath the central part (Domains 3 and 4) of the
313 moraine (MC1) complex (Figure 3). Immediately above these ramps, the sequence is repeated by a
314 number of stacked elongate (1-2 km long) thrust-bound slices of LDB sediments (Figures 3 and 8).
315 However, the presence of the ramps within this décollement suggests that thrusting also affected at
316 least the upper part of the underlying pre-Dogger Bank succession. This would have resulted in the
317 detachment and incorporation of thrust-bound blocks or glacitectonic rafts of Eem and/or Egmond
318 Ground formation sediments into the developing thrust (MC1) moraine complex. However, no

319 obvious glacitectonic rafts have been recognised due to the similar nature of the acoustic properties
320 displayed by the LDB and structurally underlying pre-Dogger Bank succession (see Figures 7 to 11).

321 In the central and northern parts of line 3 the deformed LDB is between 40 to 50 m thick
322 (Domains 3, 4 and 5; Figure 3) and contains moderately to steeply inclined reflectors which are
323 variably folded and disrupted by a series of NE-dipping, SE-directed thrusts (Figures 8 and 9).
324 Changes in fold vergence within Domain 3 (Table 2) has led to the identification of a large-scale (c. 2-
325 3 km across), upright to steeply inclined anticline. On the southern-limb of this anticline, weakly to
326 moderately developed reflectors within the LDB are deformed by NE-verging mesoscale parasitic
327 folds (see Figures 3 and 8). In contrast, on its northern-limb, the mesoscale folds once again verge
328 towards the SW, consistent with the main S/SW-direction of glacitectonic deformation. This major
329 anticline can be traced laterally across Area A where it occurs immediately to the S of the prominent
330 ramp(s) within the basal décollement surface (Figure 3) and forms a relatively flat-topped hanging-
331 wall anticline due to deformation occurring above this ramp. Domains 3, 4 and 5 record a
332 progressive increase in the relative intensity of folding and thrusting within the LDB (Figures 3, 8, and
333 9). Earlier formed thrusts within this part of the thrust-block (MC1) moraine are themselves folded,
334 indicative of a polyphase deformation history. Immediately to the N within Domain 6, the LDB is
335 acoustically "blank" with very few, if any, recognisable reflectors (see Figures 8 and 9). The
336 "massive"/"structureless" appearance may reflect the highly deformed and disrupted nature of the
337 UDB within this part of the thrust (MC1) moraine. This same progressive increase in the relative
338 intensity of deformation from Domain 3, through Domains 4 and 5, and into Domain 6 can be
339 recognised on all the seismic profiles from Area A. Importantly the blanked area occurs immediately
340 S of a prominent, arcuate basin/channel (labelled AB on Figure 2b); the latter separates the main
341 thrust complex (MC1) from a narrow ridge-like moraine (MC2) located immediately to the N (see
342 Figures 2 and 3). As a result the blanked area may represent a highly deformed zone developed
343 immediately adjacent to a former ice-contact slope with the intense disruption of the LDB possibly
344 recording a prolonged period of stillstand.

345 *5.1.2. Sedimentary architecture*

346 The locally thick UDB sequence in the southern and northern parts of Area A is typically undeformed
347 (Figure 3) with variably developed subhorizontal to inclined reflectors preserving the well-bedded
348 nature of these sediments (Figures 7 and 9). Changes in the acoustic properties of the sediments,
349 coupled with changes in dip of the reflectors has enabled the UDB to be divided into a number of
350 tabular to lenticular sedimentary "packages". Cross-cutting relationships between these packages
351 have revealed the presence of several major erosion surfaces as well as a number of channels (e.g.
352 Figures 3a and c). Bands of bright reflectors within the UDB may represent desiccation/weathering

353 surfaces within this sequence, potentially recording significant breaks in sedimentation. The
354 sedimentary packages locally possess inclined, SW-dipping bedding surfaces (foresets) (Figures 3 and
355 7). The presence of inclined foresets, the lenticular geometry and cross-cutting relationships
356 between these sediment packages suggests that they record the southward progradation of a series
357 of outwash fans or aprons. These fans/aprons would have prograded into a low-lying, proglacial
358 basin located to the S of the thrust-moraine (MC1) complex fed by meltwater channels cut into their
359 upper surfaces (see Figures 2b and 3). As noted above the lower part of the UDB sequence within
360 these aprons/fans is locally folded and thrust (Figures 3 and 7), indicating that deposition of at least
361 the early part of the UDB sequence probably accompanied glacitectonism (syntectonic
362 sedimentation). However, the well-bedded upper part of the UDB clearly overlies the highly
363 deformed sediments of the LDB (Figures 3 and 8) with the boundary between the two units being
364 interpreted as a prominent erosion surface; a conclusion supported by the presence of a thin,
365 laterally discontinuous layer of sand and gravel along the boundary between the LDB and UDB in
366 Tranche A (Cotterill *et al.*, 2017b).

367 In the northern part of the Area A, the UDB infills a 2 to 3 km wide, arcuate channel-like
368 feature (AB on Figure 2) and is variably deformed by a series of SW-verging folds and associated
369 thrusts which propagate upwards from the structurally underlying LDB (Figure 3). On Figure 9d a
370 band of bright reflectors within the UDB sequence infilling this channel is dissected by a number of
371 steeply inclined, NE-dipping faults (displacements of a few metres). However, along the northern
372 margin of Area A, the UDB sequence thickens northwards and lacks any evidence of deformation;
373 further indicating that deposition of the UDB has a complex relationship with glacitectonic
374 deformation (see Section 5).

375 **5.2. Area B**

376 *5.2.1. Structural geology*

377 The deformed Dogger Bank Formation sequence (up to c. 40 m thick) in Area B records a similar style
378 of SW-directed folding and thrusting (Domains 2, 3 and 6; Table 2) to that observed in Area A
379 (compare Figures 3 and 4). The base of the Dogger Bank sequence is once again marked by a
380 prominent subhorizontal to very gently dipping décollement surface (Figure 4). Deformation
381 accompanied the formation of a series of symmetrical to asymmetrical, thrust moraine ridges (\leq 40
382 m high) which locally possess a core of BDB enclosed within a thick carapace of LDB (Figures 4 and
383 10). The asymmetrical moraines locally possess a distinctive morphology characterised by a shorter,
384 more steeply dipping slope on their NE-side and a much longer, more gently dipping surface to the
385 SW. The shape of the buried moraines is thought to preserve the original morphology of these

386 glacitectonic landforms with their steeper NE-side potentially representing an ice-contact slope.
387 Elsewhere within Area B, however, the shape of the moraines has been strongly modified due to
388 erosion associated with the incision of a series of small (200-400 m wide) to large-scale (0.5-1 km
389 wide) channels (see Figure 2b) filled by undeformed UDB sediments (Figures 4 and 10). The top of
390 the deformed sequence is marked by a band of bright reflectors (Figure 10) consistent with this
391 former glacial land surface having undergone a period of desiccation/weathering prior to, or during
392 the early stages of the deposition of the overlying UDB. This boundary is locally offset by a series of
393 NE-dipping, SW-directed thrusts (Figure 4) indicating that periglacial weathering may have coincided
394 with at least the later stages of glacitectonic deformation.

395 *5.2.2. Sedimentary architecture*

396 The relatively thick, well-bedded UDB sequence which covers much of Area B is essentially
397 undeformed (Figure 4). Changes in the acoustic properties of the sediments, coupled with changes in
398 dip of the reflectors, have revealed the presence of a number of tabular to lenticular sedimentary
399 packages separated by prominent erosion surfaces (Figures 4 and 10). The geometry and cross-
400 cutting relationships between these sediment packages are consistent with southward progradation
401 of a series of outwash fans or aprons (see Figures 4a and b). Bands of bright reflectors within the
402 UDB (Figure 10), denoting desiccation/weathering surfaces, can be interpreted as recording
403 significant breaks in sedimentation. In contrast to Area A, the moraine (MC1) complex in Area B is
404 locally dissected by a number of large (0.5-1 km wide, 40-60 m deep), deeply incised channels which
405 have locally cut through the deformed part of the Dogger Bank Formation and into the underlying
406 pre-Dogger Bank Formation sequence (Figures 4c, 4d and 10). Marked changes in the dip of the
407 reflectors (bedding) and acoustic character of the UDB indicates that the sedimentary sequence
408 filling the channels is complex (Figure 10) and that they were probably active over a prolonged
409 period.

410 **5.3. Area C**

411 *5.3.1. Structural geology*

412 Deformation of the BDB and LDB in Area C is comparable to that recognised in the other areas
413 (compare Figures 3, 4 and 5) in that it is dominated by southerly directed folding and thrusting
414 (Domains 3 and 6; Table 2) with the base of the deformed sequence being marked by a prominent
415 subhorizontal to gently undulating décollement surface (Figure 5). However, the geometry of the
416 folds and sense of offset on the thrusts indicate that deformation in this area was directed towards
417 the SE, rather than SW as in Areas A and B. This variation in sense of shear is consistent with the
418 three study areas being located at different points around an arcuate (see Figure 2) glacitectonic
419 landform consistent with a radial pattern of ice-push resulting from an advancing, lobate ice sheet

420 margin. Local changes in the geometry (S, M and Z-shaped) meso-to small-scale (amplitudes 10 to 20
421 m) folds indicates that the LDB within the core of the moraine complex in Area C is deformed by a
422 number of large, kilometre-scale anticlines (Domain 3; Figure 5b).

423 *5.3.2. Sedimentary architecture*

424 In the northern part of Area C the deformed LDB is overlain by an undeformed sequence of UDB
425 sediments which comprise several laterally extensive tabular subunits which thicken towards the
426 NW (Figures 5a and b). A laterally extensive desiccation surface present at the top of the LDB (dark
427 purple layer on Figure 5) indicates that the surface of the moraine was exposed to periglacial
428 alteration prior to deposition of the UDB sequence. Although a clear distinction can be made
429 between the moraine complexes MC1 and MC2 on the horizon map (Figure 2) and seismic profiles
430 from Area A (Figure 3), this distinction is less apparent on the cross-sections from Area C (Figure 5).
431 The irregular upper surface of the deformed LDB forms a series of symmetrical to asymmetrical
432 ridges with the intervening small basins and/or channels (400-600 m wide) filled by essentially
433 undeformed UDB sediments (Figure 5). The lower part of this sequence, however, locally appears
434 folded or distorted as these well-bedded sediments drape the undulating, structurally controlled
435 topographic surface marking the top of the underlying deformed LDB (Figure 5c).

436 **5.4. Area D**

437 *5.4.1. Structural geology*

438 The NW-SE-trending seismic profiles (lines 12 to 15; Figure 6) from Area D provide cross-sections
439 through several of the glacitectonic moraine complexes identified within Tranche A (MC1/2, MC3
440 and MC4; Figure 2) as well as the larger sedimentary basins (Domain 8; Table 2) separating these
441 landforms. They reveal that the moraines are all composed of folded and thrust BDB and LDB, up to
442 at least 50 m thick (Figures 6 and 11). The tops of the larger moraine ridges are truncated at the
443 seabed or at the base of a thin Holocene sequence. Elsewhere the top of the LDB is marked by a
444 band of bright reflectors (e.g. Figures 11d and e); interpreted as a periglacially weathered/desiccated
445 surface (dark purple colour on Figures 6 and 11). The overall style and relative intensity of
446 deformation locally observed within the thrust-block moraines in Area D is comparable to that in the
447 other areas (compare Figures 3, 4, 5 and 6) and is once again dominated by southerly directed
448 folding and thrusting which is most apparent towards the northern-end of the cross-sections
449 (Figures 6 and 11). The S/SE-directed thrusts once again propagate upwards from a subhorizontal to
450 gently undulating décollement surface forming the base of the Dogger Bank Formation (Figure 6).
451 Although much thinner (≤ 5 -10 m thick) this deformed sequence extends beneath the sedimentary
452 basins separating the larger thrust-block moraine complexes (Figures 6 and 11). This relatively thin
453 deformed sequence locally thickens to form a number of small (10-15 m high) symmetrical to

454 asymmetrical moraine ridges composed of apparently massive/structureless (acoustically blank) UDB
455 (Domain 6; Table 2), with or without a core of BDB sediments. These smaller moraines (2-4 km wide)
456 are completely buried beneath a cover sequence of undeformed UDB (Figures 6 and 11).

457 *5.4.2. Sedimentary architecture*

458 The sedimentary basins separating the moraine complexes (MC1/2, MC3 and MC4; Figure 2) contain
459 a locally thick (up to 30-40 m) sequence of UDB well-bedded sediments (Figure 6) indicated by
460 variably developed subhorizontal to inclined reflectors (Figure 11). Changes in the acoustic
461 properties of these sediments, coupled with changes in the dip of the reflectors has enabled the
462 sequence to be once again divided into a number of tabular to lenticular sedimentary packages. On
463 Figures 6 and 11 it can be seen that the lenticular sediment packages are typically developed on the
464 SE-side (down-ice) of the moraine ridges where they form the lowest part of the UDB sequence.
465 They range in size from relatively small-scale deposits (c. 10-15 m thick, 1-2 km across; Figures 11c
466 and g) to much larger (5-10 km across; Figure 12e), internally complex sequences comprising several
467 lenticular subunits (Figures 6a and d). Inclined bedding surfaces (reflectors) within these sediment
468 packages are interpreted as foresets formed in response to the southerly progradation of these
469 deposits. These relationships support the conclusion that the lenticular sediment packages represent
470 ice-marginal fans/aprons and were formed when the ice occupied the moraine ridge. If correct it
471 would suggest that ice occupied this position for some time; once again indicating that the moraines
472 record the position of the ice margin as it retreated northwards across Dogger Bank.

473 Elsewhere within Area D the UDB basin-fill is dominated by sub-horizontally bedded,
474 laterally extensive, tabular packages of sediments (Figures 6 and 11). Cross-cutting relationships
475 between these packages record the presence of several major erosion surfaces (e.g. Figures 6a and
476 c). These surfaces are locally marked by bands of bright reflectors (e.g. Figure 11f) which represent
477 significant breaks in sedimentation enabling periglacial desiccation/weathering. In the southernmost
478 and largest basin (LB on Figures 2 and 6) a prominent, laterally extensive desiccation surface divides
479 the UDB basin-fill into two: (i) a lower, more complex sequence of lenticular to tabular sediment
480 packages which drapes the underlying glacial land surface and infills the low-lying areas between the
481 moraine ridges; (ii) overlain by an upper sequence of laterally more extensive, sheet-like sediments
482 (Figures 6 and 11). It is possible that these sheet-like sediment packages record the development of
483 a laterally more extensive outwash deposits. Cotterill *et al.* (2017b) describe the presence of loess
484 deposits and desiccation surfaces within the upper part of the Dogger Bank Formation consistent
485 with its deposition on an exposed terrestrial land surface. To the NE on line 12 the upper sequence
486 thins rapidly and locally appears to onlap onto a thick, lenticular to wedge-shaped subunit of UDB
487 sediments (Figures 6a and 11e). This subunit is interpreted as representing a 2 to 3 km wide

488 apron/fan mantling the southern side of the MC4 moraine (Figures 2 and 11) complex. The lower
489 part of this apron/fan sequence is deformed by a series of open, upright folds and faults which
490 propagate upwards from the underlying deformed LDB (Figures 6 and 11e), suggesting that
491 glacitectonic deformation may have accompanied the deposition of the lower part of the UDB.

492

493 **6. Model of active ice retreat resulting in large-scale glacitectonic** 494 **deformation**

495 Although in detail the style and relative intensity of deformation recorded by the BDB, LDB and, to a
496 lesser extent, UDB varies across the Tranche A (Figure 3 to 6) a number of general observations can
497 be made regarding the glacitectonic deformation of the Dogger Bank Formation:

- 498 • The deformed sediments dominating the lower part of the Dogger Bank Formation form a
499 series of ridge-like landforms (individual ridges 0.5-3 km wide, up to 40 m high) composed of
500 folded and thrust BDB and LDB. These glacitectonic landforms can be traced laterally for
501 several hundred metres to kilometres forming arcuate, linear bodies within the larger thrust-
502 block moraine complexes or composite ridges (MC1 to MC4; Figure 2) (as defined by Benn
503 and Evans, 2010), the largest of which (MC1) is up to 15-20 km across;
- 504 • Glacitectonic deformation is dominated by southerly-directed folding and thrusting (Figures
505 3 to 11) consistent with it having been driven by ice advancing from the N/NW. The variation
506 in the direction of shear from towards the SW in Area A, through to SE in Area D is
507 consistent with a radial pattern of ice-push resulting in ice-marginal to proglacial
508 deformation in front of the advancing, lobate ice sheet margin;
- 509 • The base of the deformed sequence is marked by a prominent, laterally extensive
510 d collement surface (Figures 3 to 6) which modified/overprinted the original stratigraphical
511 relationship(s) between the Dogger Bank Formation and the underlying pre-Dogger Bank
512 Formation sequence. Locally developed ramps indicate that thrusting may have affected the
513 upper part of the underlying pre-Dogger Bank succession;
- 514 • The thickness of the BDB is highly variable with this structurally lowest unit within the
515 Dogger Bank Formation locally forming the cores to the larger thrust-block moraines (Figures
516 3 to 6). A prominent periglacial desiccation/weathering surface at the top of the unit is
517 deformed indicating that deposition of the BDB and its subsequent glacitectonism were
518 separated by a potentially significant time gap;

- 519 · The tops of the larger thrust-block moraine complexes (Benn and Evans, 2010) are locally
520 truncated (eroded) at the sea bed or at the base of a thin sequence of undeformed UDB
521 and/or Holocene sediments. Elsewhere the top of the deformed LDB sequence is marked by
522 a desiccation surface indicating that the moraines underwent a period of periglacial
523 weathering/alteration and/or erosion prior to the deposition of the UDB;
- 524 · The UDB is in general undeformed suggesting that deposition of these sediments largely
525 post-dated glacitectonism. Locally, however, folding and thrusting can be seen to propagate
526 upwards from the underlying LDB to affect the overlying UDB, indicating that deposition of
527 at least the lower part of the UDB accompanied deformation. Elsewhere (e.g. Area B) the
528 moraines are deeply incised by a series of meltwater channels filled by undeformed UDB
529 sediments; and
- 530 · The UDB can be divided into two main subunits: (i) a lower, more complex succession of
531 lenticular to tabular sediment packages which drape the underlying land surface and infill
532 the low-lying areas between the moraine ridges; and (ii) an overlying succession composed
533 of laterally extensive, sheet-like sediment packages (Figures 3 to 6). Lenticular to wedge-
534 shaped sediment packages within the UDB are interpreted as southerly prograding fans or
535 aprons mantling the distal (down-ice) side of the moraines. Whereas the sheet-like sediment
536 packages record the subsequent development of a more laterally extensive outwash
537 deposits.

538 Consequently the simplest model for the construction of the thrust-block moraines (MC1 to MC4;
539 Figure 2) identified on the Dogger Bank is one of ice-marginal to proglacial deformation resulting
540 from ice-push associated with the repeated advance of a lobate ice-margin from the N/NW.
541 Although the shape of these glacitectonic landforms has locally been modified as a result of erosion
542 accompanying the deposition of the overlying UDB sequence, there is no evidence to suggest that
543 the thrust-block moraines have been overridden. Consequently the phases of ice sheet advance
544 responsible for the large-scale glacitectonic deformation are thought to have occurred during an
545 overall pattern of ice sheet retreat (deglaciation) from the Dogger Bank (see Section 6.2). Deposition
546 of the deformed lower part of the UDB occurred whilst the ice sheet occupied the individual ice
547 limits represented by the thrust-block moraines, forming a series of lenticular aprons/fans which
548 prograded southward into the adjacent ice-marginal to proglacial sedimentary basins. The
549 undeformed, tabular to sheet-like deposits which characterise the upper part of the UDB are
550 considered to represent laterally more extensive outwash deposits laid down as the ice sheet
551 retreated northward.

552 **6.1. Construction of large, thrust moraine complexes as a result of glacitectonic**
553 **deformation at an oscillating ice sheet margin**

554 The largest of the thrust-block moraine complexes (MC1; Figure 2) identified within Tranche A (Areas
555 A to D) is in the order of 15-20 km across and can be traced laterally for over 40 to 50 km. Cross-
556 sections through this thrust-block moraine system (lines 1 to 4; Figure 3) reveal that it is internally
557 structurally complex (see Section 5.1) and composed of a large volume of highly deformed
558 sediments (Figures 3, 7, 8 and 9). The large scale of this thrust-block moraine, coupled with the
559 observed marked changes in structural style and relative intensity of deformation of the deformed
560 sequence enabling it to be divided into a series of structural domains (c.f. Cotterill *et al.*, 2017a), as
561 well as evidence for the polyphase deformation (e.g. folding of earlier developed thrusts in response
562 to later deformation) and the presence of a deformed channel-fill sequence included within the
563 landsystem (Figure 3) indicate that this complex glacitectonic landform did not form as a result of a
564 single phase of ice-push. Furthermore, cross-cutting relationships between the individual ridge-like
565 features identified within this thrust-block moraine (Figure 2b) are also consistent with this complex
566 landforms having been constructed in response to several phases of ice advance (Stages 1 to 9;
567 Figure 12). Consequently, the individual thrust-block moraine complexes (MC1 to MC4; Figure 2) are
568 not the product of a single phase of ice sheet advance, but evolved over a prolonged period and
569 resulted several phases of readvance during which the ice sheet repeatedly reoccupied essentially
570 the same ice limit. Each readvance would have been followed by a phase of retreat, accompanied by
571 the deposition of an outwash sequence laid down within an ice-marginal to proglacial sedimentary
572 basin which opened between the rear of the evolving moraine complex and the retreating ice
573 margin (Stages 3, 5 and 7; Figure 12). During the following readvance these outwash sediments
574 would have been deformed (folded and thrust) and accreted onto the up-ice side of the evolving
575 moraine complex (Figure 12). This interpretation is supported by the similar acoustic properties
576 displayed by the deformed LDB and undeformed UDB sequences (see Figures 7 to 11). Furthermore,
577 boreholes through the Dogger Bank Formation reveal that both units are composed of lithologically
578 similar sequences of stiff to very stiff clays containing multiple sand interbeds (Cotterill *et al.*,
579 2017b). Consequently, these large-scale thrust moraine complexes owe their origins to the complex
580 interplay between glacitectonism and penecontemporaneous sedimentation at a highly dynamic,
581 oscillating ice sheet margin.

582 The model proposed for the evolution of the largest of the internally complex glacitectonic
583 landforms on Dogger Bank is shown in Figure 12. During the initial phase of ice sheet advance the ice
584 is thought to have overridden the BDB sequence (Stage 1; Figure 12). This basal unit was deposited
585 prior to the development of the glacitectonic landsystem which characterises the Dogger Bank
586 Formation within Tranche A. The presence of a well-developed desiccation surface at the top of the

587 BDB indicates that Dogger Bank was subaerially exposed (c.f. Cotterill *et al.*, 2017b) and this
588 terrestrial land surface was subjected to a period of periglacial weathering and alteration prior to its
589 inundation by ice. The presence of BDB sediments across Tranche A can be used to suggest that the
590 advancing ice sheet may have been decoupled from its bed facilitating the preservation of these
591 mud-rich sediments beneath the overriding ice mass (Stage 1; Figure 12). However at some point
592 during this advance the ice began to couple with its bed, possibly due to the dewatering of the ice-
593 bed interface leading to a reduction in basal sliding and transmission of increasing amounts of shear
594 into the underlying BDB. Coupling of the ice to its bed initially led to the development of a forward
595 propagating imbricate thrust stack (Stage 2; Figure 12). This southerly propagating thrust system is
596 preserved along the southern margin of the MC1 moraine complex in Area A (Domain 1; Figure 3).
597 The propagation of the basal décollement into the forefield in advance of ice sheet would lead to the
598 sequential detachment of progressively “younger” (structurally) thrust-bound slices of BDB
599 sediments. These detached slabs were accreted to the base of the evolving imbricate stack leading
600 to the “back-rotation” (i.e. northward sense of rotation of the detached thrust-bound slab is towards
601 the advancing ice sheet) of structurally higher and older thrust-slices; the latter becoming
602 increasingly steeper in attitude towards the ice margin (Figures 3 and Stage 2 on 12). As the ice sheet
603 continued to advance the deforming BDB would have accommodated a greater degree of
604 shortening, reflected in the increasing complexity and relative intensity of deformation northwards
605 towards the ice margin (Figures 3 and Stage 2 on 12). Furthermore the progressive accretion, back-
606 rotation and up-thrusting of successively younger thrust-bound slabs of BDB may have resulted in an
607 increase in the surface topography (height) of the evolving thrust-block moraine. At some point
608 forward motion of the ice mass is thought to have ceased due to either: the “locking up” of the
609 imbricate thrust stack; the size of this evolving landform reaching a “critical mass” so that it acted as
610 a “buffer” preventing further ice sheet advance; and/or a change in ice sheet dynamics.

611 The ice sheet appears to have remained at this maximum position for some time allowing
612 the deposition of a sequence of UDB outwash sediments mantling the upper surface of the moraine
613 (Stage 2; Figure 12). Minor oscillations in the position of the ice margin whilst it was at this stillstand
614 position may have resulted in the penecontemporaneous deformation of the recently deposited
615 outwash. The ice mass subsequently underwent a phase of retreat laying down sediments in a
616 temporary sedimentary basin which opened between the moraine and the retreating ice margin
617 (Stage 3; Figure 12). A subsequent readvance led to the deformation of these recently deposited
618 sediments and their accretion onto the up-ice side of the moraine complex (Stage 4; Figure 12). This
619 cycle of sedimentation during ice sheet retreat followed by glacitectonic deformation in response to
620 a readvance is thought to have occurred a number of times (Stages 5 to 9; Figure 12) resulting in the

621 observed structurally complexity within the thrust moraine system. This model can be applied to all
622 of the moraine complexes within Tranche A (MC1 to MC4) with the individual ridges identified on
623 the horizon and landform maps (Figure 2) marking the readvance positions of the ice sheet margin
624 during their construction. The accretion of progressively younger thrust-sheets onto the up-ice side
625 of the evolving moraine complex may have led to the localised reactivation and/or folding of earlier
626 developed structures (e.g. thrusts; see Figure 3) resulting in the locally observed polyphase
627 deformation history recorded by the LDB and large-scale folding within the cores of the moraine
628 complexes. Apparently structureless (acoustically blank) sections within the moraine complex
629 (Figures 7 to 9) are considered to represent highly disrupted parts of the LDB sequence resulting
630 from locally intense deformation adjacent to former ice-contact slopes.

631 **6.2. Factors controlling the location and development of the décollement surface at the** 632 **base of the Dogger Bank Formation**

633 The laterally extensive subhorizontal to very gently dipping décollement surface marking the base of
634 the Dogger Bank Formation is apparently developed at essentially the same stratigraphic/structural
635 level across Tranche A (Areas A to D; Figures 3 to 6). A number of previous studies have argued that
636 proglacial to ice marginal thrusting can be facilitated by the introduction of pressurised meltwater
637 along evolving thrust planes (Bluemle and Clayton, 1983; Ruszczynska-Szenajch, 1987, 1988; Phillips
638 *et al.*, 2008; Phillips and Merritt, 2008; Burke *et al.*, 2009). For example Vaughan-Hirsch and Phillips
639 (2016) and Phillips *et al.* (2017) have suggested that the décollement surface at the base of large-
640 scale imbricate thrust stacks which deform the Aberdeen Ground Formation of the central North Sea
641 and Cretaceous bedrock at the Mud Buttes, southern Alberta (Canada), respectively, formed in
642 response to the over-pressurisation of the groundwater system during rapid ice sheet advance
643 (surge-type behaviour). These authors argue that the resulting increase in the hydrostatic gradient
644 would force groundwater from beneath the ice sheet (higher overburden pressure) into its forefield
645 (lower pressure) (Boulton and Caban, 1995), facilitating the propagation of this detachment in front
646 of the advancing ice mass.

647 A similar model could be applied to the Dogger Bank thrust moraines where surge-type
648 behaviour could lead to a rapid advance of the ice sheet lobe and pressurisation of groundwater
649 within the underlying Quaternary sediments. The lithological contrast between the sands of the
650 Eem/Egmond Ground formation(s) at the top of the underlying sequence and the Dogger Bank
651 Formation may have resulted in the focusing of this pressurised groundwater along this major
652 lithostratigraphic boundary. The mud-rich BDB sediments would have acted as an aquitard trapping
653 water beneath the ground surface and within the upper part of the Eem/Egmond Ground formation.
654 The trapping and localisation of pressurised groundwater at this boundary may have been further

655 aided by the presence of a well-established permafrost layer at the top of the BDB; evidence for this
656 layer being provided by the laterally extensive desiccation surface developed at the top of this unit
657 (see Figures 3 to 11). The resultant increase in pore water pressure within the unconsolidated
658 Eem/Egmond Ground formation sands could have led to a lowering of their cohesive strength,
659 leading to failure and propagation of a water-lubricated décollement out into the forefield. Once
660 formed, this essentially bedding-parallel detachment would have represented an ideal fluid
661 pathway, helping to transmit pressurised water further into the forefield, leading to “thrust gliding”
662 (Nieuwland *et al.*, 2000; Mourgues *et al.*, 2006) and facilitating transmission of shear in front of the
663 advancing ice sheet.

664

665 **7. Active retreat of a Weichselian ice sheet from Dogger Bank**

666 It is clear from the above that rather than being a stratigraphically simple “layer-cake” composed of
667 stratified to well-bedded sediments deposited in proglacial or glaciolacustrine setting (Cameron *et al.*, 1992) the Dogger Bank Formation is far more complex. Concealed beneath an undeformed
668 sequence of outwash sediments (UDB) and Holocene to recent deposits is evidence of a buried
669 glacitectonic landsystem (cf. Cotterill *et al.*, 2017a, b), comprising large (up to 40-50 m high, 15-20
670 km across, over 40-50 km in length) arcuate thrust-block moraine complexes separated by low-lying
671 sedimentary basins (Figure 2). Comparable large-scale glaciotectonic complexes comprising folded
672 and thrustured glacial sediments have been described elsewhere within the North Sea Basin and
673 adjacent areas where they are associated with glaciations of different ages (e.g. Huuse *et al.*, 2001;
674 Andersen *et al.*, 2005; Phillips *et al.*, 2008; Burke *et al.*, 2009; Bakker and van der Meer, 2015;
675 Vaughan-Hirsch and Phillips, 2017; Lee *et al.*, 2013, 2017; Pedersen and Boldreel 2017). Prominent
676 desiccation surfaces developed at the tops of the BDB and LDB, and within the UDB which are
677 interpreted as having formed in response to intense periglacial weathering/alteration clearly
678 indicate that this was a subaerially exposed, terrestrial landscape (cf. Cotterill *et al.*, 2017b). The
679 internal structural complexity of the glaciotectonic landforms has led to the conclusion that their
680 construction occurred at a highly dynamic, oscillating ice sheet margin which repeatedly readvanced
681 and reoccupied a series of recessional ice limits (Figure 12). The result of this model is that the
682 relative age of the deformation recorded by the BDB/LDB sequences and depositional age of the
683 overlying UDB outwash sediments is diachronous; both become progressively younger towards the
684 N/NW across Tranche A. The construction of comparable regionally extensive glaciotectonic
685 landsystems (Neutral Hills, Sharp Hills, Misty Hills, Mud Buttes) have been associated with the surge-
686 like activity within the Prospect Valley lobe of the Central Alberta Ice Stream (Canada). This phase of
687

688 highly dynamic activity within the Prospect Valley lobe occurred during the overall northward retreat
689 of the Laurentide Ice Sheet across Alberta (Evans *et al.*, 2008, 2014; O’Cofaigh *et al.*, 2010; Atkinson
690 *et al.*, 2014; Phillips *et al.*, 2017) and links large-scale glacitectorism to fast ice flow. A similar model
691 of surge-related large-scale glacitectorism during the retreat of an oscillating ice sheet margin can
692 be applied to the Dogger Bank area of the North Sea (Figure 13).

693 The glacitectonic landsystem (MC1 to MC4, Figure 2) preserved within the Dogger Bank
694 Formation comprises a network of anastomosing, arcuate to locally cross-cutting moraine-ridges
695 separated by large ice-marginal to proglacial sedimentary basins (e.g. LB on Figure 2). The presence
696 of this landsystem provides unequivocal evidence that, at its maximum extent, the Weichselian ice
697 sheet not only inundated the Dogger Bank, but probably extended further south into the North Sea
698 basin; supporting the postulated ice limits within the southern North Sea proposed by Jansen *et al.*
699 (1979), Carr *et al.* (2006), Boulton and Hagdorn (2006), Hubbard *et al.* (2009), Graham *et al.* (2011)
700 and Sejrup *et al.* (2016) amongst others (see Figure 1a). Furthermore, no evidence has been found to
701 suggest that the moraine ridges have been overridden during a later glaciation suggesting that this
702 complex landsystem was formed during the Last Glacial Maximum (LGM). The large thrust moraine
703 complexes within Tranche A (M1 to M4; Figure 2) are interpreted as delineating recessional ice limits
704 formed in response to the repeated readvance of a highly dynamic, lobate ice margin, occurring
705 during the overall northward (N/NW) retreat of the Weichselian ice sheet from this part of the North
706 Sea. This retreat history is illustrated on Figure 13 where the progressive changes in the shape and
707 positions of the ice sheet margin have been established using the morphology of the moraine-ridges
708 (Figure 2b). Due to the lack of published seismic data, no attempt has currently been made to
709 project the ice margin to the south and east of Tranche A. However, based on the evidence from this
710 data set the ice margin is thought to have extend further to the south of the DBZ.

711 The largest moraine complex (MC1; Figures 2 and 13) marks the most southerly position of
712 the Weichselian ice sheet within Tranche A; although, at its maximum extent, the ice is likely to have
713 extended further to the S (see Figure 2a). The ice sheet clearly repeatedly reoccupied this position
714 over a prolonged period (Figures 13a to f) resulting in the construction of this internally complex, 15-
715 20 km wide glacitectonic landform. Its construction was accompanied by the deposition of an UDB
716 outwash sequence which formed a series of southerly prograding aprons or fans mantling the down-
717 ice side of the moraine complex (Figure 12). Meltwater expelled from the retreating ice incised a
718 network of small to locally large-scale drainage channels (see Figure 2b) which locally modified the
719 shape of the evolving moraine complex (Area B; Figure 4). Although there is likely to have been
720 localised ponding of meltwater between the evolving moraine ridges and at the ice margin, the

721 incision of deep (up to 40 to 60 m; see Figures 4 and 10) drainage channels which cut through the
722 MC1 moraine will have drained the area adjacent to the ice sheet margin (Figure 13), effectively
723 preventing the establishment of the large proglacial lake (at least in this part of the Dogger Bank)
724 proposed by Cameron *et al.* (1992) (also see Valentin 1955; Veenstra 1965; Cohen *et al.*, 2014; Hijma
725 *et al.*, 2012; Murton and Murton, 2012; Sejrup *et al.*, 2016). This conclusion is supported by the
726 occurrence of several well-developed, regionally extensive desiccation surfaces within the Dogger
727 Bank Formation of Tranche A providing unequivocal evidence that this part of Dogger Bank was a
728 subaerially exposed terrestrial land surface and subject to repeated phases of periglacial weathering
729 and alteration (Cotterill *et al.*, 2017b). Eventually the ice sheet retreated northward leaving the MC1
730 and MC2 moraine complexes separated by an arcuate, elongate basin or channel (Figures 2 and 13)
731 filled by variably deformed UDB outwash (Figure 3). The shape of the arcuate moraine ridges within
732 both of these complexes, coupled with the kinematics obtained from the glacitectonic structures
733 indicates that ice sheet movement at this stage of the retreat history was predominantly N/NNW-
734 S/SSE (Figure 13a to e).

735 Following the accretion of MC2 moraine complex onto the up-ice side of the much larger
736 MC1 system (Figure 13e) the Weichselian ice sheet is thought to have retreated further N (Figure
737 13f). Its subsequent readvance into Tranche A was less extensive and led to the construction of the
738 outer, southernmost moraine-ridges of the MC3 complex (Figure 13i). The large, low-lying basin
739 formed between the MC1/2 and MC3 moraines (LB on Figure 2) was progressively filled by a
740 sequence of UDB outwash sediments (Figure 6). This sequence includes a series of fans/aprons
741 developed on the down-ice side of the MC3 moraine complex which prograded southwards into the
742 basin. These sediments were locally deformed as the ice repeatedly reoccupied the MC3-limit
743 building up a series of arcuate moraine ridges separated by small ice-marginal/proglacial basins
744 (Figures 2 and 13h to i) filled by penecontemporaneous outwash (Figure 6). At its southwestern-end
745 the MC3 moraine clearly crosscuts and truncates the earlier formed MC1 and MC2 systems (Figures
746 2 and 13g). Furthermore, the shape of the MC3 moraine is more consistent with it having been
747 constructed by ice advancing from the NW (Figure 3i) rather than the predominantly N-S sense of
748 movement established for the earlier part of the retreat history (Figure 13). A prominent
749 desiccation/weathering surface within the UDB sequence (see Figure 6) filling the proglacial basin
750 (LB on Figure 3) represents a break in sedimentation; possibly coinciding with one of the
751 readvances/oscillations responsible for the construction of the MC3 moraine. Meltwater production
752 and associated sedimentation within the proglacial area is likely to be lower during ice sheet
753 advance enabling the development of permafrost within the forefield.

754 The final phase of readvance of the Weichselian ice sheet into Tranche A was apparently
755 more localised in extent and led to the construction of the MC4 moraine (Figure 13j). The shape of
756 the moraine-ridges within this complex once again suggests that the main ice-movement direction
757 was from the NW. This change from a N-S (MC1 and MC2 moraines) to more NW-SE (MC3 and MC4
758 moraines) direction of ice-movement (see Figure 13) during the northwards retreat of the
759 Weichselian ice sheet suggests that there was a significant change in the structural configuration of
760 this ice mass during deglaciation. Furthermore the size and spacing between the individual moraine-
761 ridges within these larger glacitectonic moraine complexes varies from S to N across Tranche A. The
762 ridges within the MC3 and MC4 moraines are relatively smaller and more widely spaced than the
763 tightly packed landforms present within the structurally more complex MC1 moraine (Figure 2). This
764 decrease in size and increase the spacing of the glacitectonic landforms northward across Tranche A
765 is thought to record an overall decrease in the magnitude of the readvances/oscillations responsible
766 for the construction of these glacitectonic landforms. Comparable relationships between the size
767 and spacing of annual recessional moraines formed during the recent retreat histories of
768 contemporary Icelandic glaciers, reflecting changes in the magnitude of the winter/spring
769 readvance, have been described by several authors (e.g. Evans and Twigg, 2002; Bradwell *et al.*,
770 2013; Phillips *et al.*, 2014). The geomorphological record preserved within the Dogger Bank
771 Formation is therefore thought to not only record a significant change in the structural configuration
772 of Weichselian ice sheet, but also the progressive weakening of this ice mass as it retreated
773 northwards.

774 The N-S to NW-SE direction of ice movement derived from the landforms and glacitectonic
775 deformation structures preserved within the Dogger Bank Formation is consistent with the regional-
776 scale pattern ice flow derived from the ice sheet modelling of Boulton and Hagdorn (2006) and the
777 reconstruction for Weichselian ice sheet within the North Sea basin of Sejrup *et al.* (2016). Both of
778 these approaches suggest that at its maximum (i.e. when the BIIS and FIS were confluent forming a
779 single ice mass) and during the initial stages of collapse, the Weichselian ice inundating Dogger Bank
780 would have been flowing S/SSE from an approximately E-W-trending ice divide linking NE Scotland
781 and southern Norway (see fig. 10 of Boulton and Hagdorn, 2006 and fig. 3 of Sejrup *et al.*, 2016).
782 Furthermore the model simulations of Boulton and Hagdorn (2006) also predict relatively fast ice
783 flow across the Dogger Bank region, supporting the proposed model for the construction of the
784 Dogger Bank moraine complex as having occurred in response to large-scale glacitectonics during
785 surge-related marginal readvance as the Weichselian ice sheet retreated northwards from the
786 southern central North Sea.

787

788 **8. Conclusions**

789 The detailed analysis of high-resolution seismic data from the Dogger Bank in the southern central
790 North Sea has revealed that the Dogger Bank Formation records a complex history of sedimentation
791 and penecontemporaneous, large-scale, ice-marginal to proglacial glacitectorism associated with
792 the active retreat of the Weichselian ice sheet. The 2D seismic profiles provide a series of cross-
793 sections through a large thrust moraine complex which is buried beneath a thin sequence of
794 Holocene sediments. This glacitectoric landsystem comprises a series of elongate, arcuate moraine-
795 ridges separated by low-lying ice marginal to proglacial sedimentary basins and/or meltwater
796 channels, preserving the shape of the former ice sheet margin. The individual moraines, the largest
797 of which is up to 15-20 km across, are composed of folded and thrust sediments belonging to the
798 basal and lower units of the Dogger Bank Formation. Deformation was dominated by southerly-
799 directed folding and thrusting, with glacitectorism having been driven by ice advancing from the
800 N/NW. The base of the deformed sequence is marked by a prominent, laterally extensive
801 *décollement* surface which modified the original stratigraphical relationship(s) between the Dogger
802 Bank Formation and the underlying sequence. The upper part of the Dogger Bank Formation is in
803 general undeformed; suggesting that deposition of these sediments largely post-dated
804 glacitectorism and that they were laid down as a series of ice-marginal fans/aprons and sheet-like
805 sandur deposits which prograded southwards into the adjacent proglacial sedimentary basins
806 located between the moraines. The internal structural architecture of the Dogger Bank thrust
807 moraine complexes can be directly related to ice sheet dynamics, recording the former positions of
808 an highly dynamic, oscillating Weichselian ice sheet margin as it retreated northwards at the end of
809 the Last Glacial Maximum.

810

811 **9. Acknowledgements**

812 The authors would like to thank the Forewind Consortium (Statoil, Statkraft, RWE and SSE) for their
813 permission to use the datasets acquired during surveys conducted for licensing purposes. In addition
814 we thank colleagues at British Geological Survey, Norwegian Geotechnical Institute and RPS
815 including Claire Mellett, Gareth Carter, Carl Fredrik Forsberg, Tor Inge Yetginer-Tjelta, Tom Lunne,
816 Don de Groot, Oyvind Blaker, David Long, Callum Duffy and Dayton Dove. Heather Stewart is
817 thanked for her comments on an earlier version of this manuscript. Stig Schack Pedersen is thanked
818 for his constructive review of our paper. This paper is published with permission of the Executive
819 Director of the British Geological Survey, Natural Environmental Research Council.

820

821 **10. References**

822 Andersen, L.T., Hansen, D.L., Huuse, M. 2005. Numerical modelling of thrust structures in
823 unconsolidated sediments: implications for glaciotectionic deformation. *Journal of Structural Geology*
824 **27**, 587-596.

825 Atkinson, N., Utting, D.J., Pawley, S.P. 2014. Landform signature of the Laurentide and Cordilleran ice
826 sheets across Alberta during the last glaciation. *Canadian Journal of Earth Sciences* **51**, 1067-1083.

827 Bakker, M.A.J., van der Meer, J.J.M. 2003. Structure of a Pleistocene push-moraine revealed by
828 ground-penetrating radar: the eastern Veluwe Ridge, the Netherlands. In: Bristow, C.S., Jol, H.M.
829 (Eds.), Ground Penetrating Radar in Sediments. *Geological Society of London Special Publications*,
830 **211**, 143-151.

831 Balson, P.S., Cameron, T.D.G. 1985. Quaternary mapping offshore East Anglia. *Marine Geology* **9**, pp.
832 221-239

833 Beets, D.J., Meijer, T., Beets, C.J., Cleveringa, P., Laban, C., van der Spek, A.J.F. 2005. Evidence for a
834 Middle Pleistocene glaciation of MIS 8 age in the southern North Sea. *Quaternary International* **133-**
835 **134**, 7-19.

836 Belt, T. 1874. An examination of the theories that have been proposed to account for the climate of
837 the glacial period. *Quarterly Journal of Science*, 421-464.

838 Benn, D.I., Evans, D.J.A. 2010. *Glaciers and Glaciation*. Arnold, London, U. K. 802 pp.

839 Bluemle, J.P., Clayton, L. 1983. Large-scale glacial thrusting and related processes in North Dakota.
840 *Boreas* **13**, 279-299.

841 Boulton, G.S., Caban, P. 1995. Groundwater flow beneath ice sheets, part II; Its impact on glacier
842 tectonic structures and moraine formation. *Quaternary Science Reviews* **14**, 563-587.

843 Boulton, G.S., Hagdorn, M. 2006. Glaciology of the British Isles Ice Sheet during the last glacial cycle:
844 Form, flow, streams and lobes. *Quaternary Science Reviews* **25**, 3359-3390.

845 Bradwell, T., Stoker, M.S., Gollledge, N.R., Wilson, C.K., Merritt, J.W., Long, D., and others. 2008. The
846 northern sector of the last British Ice Sheet: maximum extent and demise. *Earth Science Reviews* **88**,
847 207-226.

- 848 Bradwell, T., Sigurdsson, O., Everest, J. 2013. Recent, very rapid retreat of a temperate glacier in SE
849 Iceland. *Boreas* **42**, 959–973.
- 850 British Geological Survey and Rijks Geologische Dienst. 1989. Silver Well Quaternary Geology. 1:250
851 000. Keyworth, Nottingham: British Geological Survey.
- 852 British Geological Survey and Rijks Geologische Dienst. 1991. Dogger Quaternary Geology. 1:250
853 000. Keyworth, Nottingham: British Geological Survey.
- 854 Brooks, A.J., Bradley, S.L., Edwards, R.J., Milne, G.A., Horton, B., Shennan, I. 2008. Postglacial relative
855 sea-level observations from Ireland and their role in glacial rebound modelling. *Journal of*
856 *Quaternary Science* **23**, 175–192.
- 857 Burke, H., Phillips, E., Lee, J.R., Wilkinson, I.P. 2009. Imbricate thrust stack model for the formation of
858 glaciotectionic rafts: an example from the Middle Pleistocene of north Norfolk, UK. *Boreas* **38**, 620-
859 637.
- 860 Cameron, T.D.J., Stoker, M.S., Long, D. 1987. The history of Quaternary sedimentation in the UK
861 sector of the North Sea Basin. *Journal of the Geological Society, London* **144**, 43-58.
- 862 Cameron, T.D.J., Crosby, A., Balson, P.S., Jeffery, D.H., Lott, G.K., Bulat, J., Harrison, D.J. 1992. *United*
863 *Kingdom offshore regional report: the geology of the southern North Sea*. London: HMSO for the
864 British Geological Survey.
- 865 Carr, S.J., Holmes, R., van der Meer, J.J.M., Rose, J. 2006. The Last Glacial Maximum in the North Sea
866 Basin: micromorphological evidence of extensive glaciation. *Journal of Quaternary Science* **21**, 131-
867 153.
- 868 Caston, V.N.D. 1977. A new isopachyte map of the Quaternary of the North Sea. *Institute of*
869 *Geological Sciences Report* **10 (11)**, 3–10.
- 870 Caston, V.N.D. 1979. The Quaternary sediments of the North Sea. In: Banner, F.T., Collins, M.B.,
871 Massie, K.S. (eds) *The North-West European shelf seas: The sea bed and the sea in motion*. 1.
872 Geology and Sedimentology. Elsevier, New York. 195–270.
- 873 Catt, J.A. 1991. Late Devensian glacial deposits and glaciations in eastern England and the adjoining
874 offshore region. In: Ehlers J, Gibbard PL, Rose J (eds) *Glacial Deposits in Great Britain Ireland*. A.A.
875 Balkema: Rotterdam. 61–68.

- 876 Cohen, K.M., Gibbard, P.L., Weerts, H.J.T. 2014. North Sea palaeogeographical reconstructions for
877 the last 1 Ma. *Geologie en Mijnbouw* **93**, 7-29.
- 878 Cotterill, C.J., Phillips, E., James, L., Forsberg, C.F., Tjelta, T.I. 2017a. How understanding past
879 landscapes can inform present day site investigations: A case study from Dogger Bank, southern
880 central North Sea. *NSG Marine Special Publication*.
- 881 Cotterill, C.J., Phillips, E., James, L., Forsberg, C.F., Tjelta, T.I., Dove, D. 2017b. The evolution of the
882 Dogger Bank, North Sea: a complex history of terrestrial, glacial and marine environmental change.
883 *Quaternary Science Reviews*.
- 884 Clark, C.D., Evans, D.J.A., Khatwa, A., Bradwell, T., Jordan, C.J., Marsh, S.H., Mitchell, W.A., Bateman,
885 M.D. 2004. Map and GIS database of glacial landforms and features related to the last British Ice
886 Sheet. *Boreas* **33**, 359-375.
- 887 Cotterill, C., Phillips, E., James, L., Forsberg, C.F. Tjelta, T.I. 2017a. How understanding past
888 landscapes can inform present day site investigations: A case study from Dogger Bank, southern
889 central North Sea. *NSG Marine Special Publication*.
- 890 Cotterill, C.J., Phillips, E., James, L., Forsberg, C.F., Tjelta, T.I., Carter, G., Dove, D. 2017b. The
891 evolution of the Dogger Bank, North Sea: a complex history of terrestrial, glacial and marine
892 environmental change. *Quaternary Science Reviews*.
- 893 Davis, D., Suppe, J., Dahlen, F.A. 1984. Mechanics of fold-and-thrust belts and accretionary wedges:
894 Cohesive Coulomb theory. *Journal of Geophysical Research* **89**, 10087-10101.
- 895 Dunlop, P., Shannon, R., McCabe, M., Quinn, R., Doyle, E. 2010. Marine geophysical evidence for ice
896 sheet extension and recession on the Malin Shelf: New evidence for the western limits of the British
897 Irish Ice Sheet. *Marine Geology* **276**, 86-99.
- 898 Eisma, D., Jansen, J.H.F., van Weering, T.C.E. 1979. Sea floor morphology and recent sediment
899 movement in the North Sea. In: Oele, E., Schuttenhelm, R.T.E., Wiggers, A.J. (eds) The Quaternary
900 history of the North Sea. Acta Univ. Ups. Symposium. Univ. Ups Annum Quintegentesimum
901 Celebrantis, Uppsala. 217-231.
- 902 Ehlers, J., 1990. Reconstructing the dynamics of the north-west European Pleistocene ice sheets.
903 *Quaternary Science Reviews* **9**, 71-83.
- 904 Evans, D.J.A., Twigg, D.R. 2002. The active temperate glacial landsystem: a model based on
905 Breiðamerkurjökull and Fjallsjökull, Iceland. *Quaternary Science Reviews* **21**, 2143–2177.

- 906 Evans, D.J.A., Clark, C.D., Rea, B.R. 2008. Landform and sediment imprints of fast glacier flow in the
907 southwest Laurentide Ice Sheet. *Journal of Quaternary Science* **23**, 249–272.
- 908 Evans, D.J.A., Young, N.J., Cofaigh, C. 2014. Glacial geomorphology of terrestrial terminating fast flow
909 lobes/ice stream margins in the southwest Laurentide ice sheet. *Geomorphology* **204**, 86–113.
- 910 Gatliff, R.W., Richards, P.C., Smith, K., Graham, C.C., McCormack, M., Smith, N.J.P., Jeffery, D., Long,
911 D., Cameron, T.D.J., Evans, D., Stevenson, A.G., Bulat, J., Ritchie, J.D. 1994. United Kingdom offshore
912 regional report: the geology of the central North Sea. London: HMSO for the British Geological
913 Survey.
- 914 Glennie, K.W., Underhill, J.R., 1998. Origin, development and evolution of structural styles. In:
915 Glennie, K.W. (ed.) *Petroleum Geology of the North Sea: Basic Concepts and Recent Advances*
916 (fourth edition). Blackwell Science Ltd., Oxford, 42-84.
- 917 Graham, A.G.C., Lonergan, L., Stoker, M.S. 2007. Evidence for Late Pleistocene ice stream activity in
918 the Witch Ground Basin, central North Sea, from 3D seismic reflection data. *Quaternary Science*
919 *Reviews* **26**, 627-643.
- 920 Graham, A.G.C., Lonergan, L., Stoker, M.S. 2010. Depositional environments and chronology of Late
921 Weichselian glaciation and deglaciation in the central North Sea. *Boreas* **39**, 471–491.
- 922 Graham, A.G.C., Stoker, M.S., Lonergan, L., Bradwell, T., Stewart, M.A., 2011. The Pleistocene
923 glaciations of the North Sea Basin. In: Ehlers, J., Gibbard, P.L. (eds) *Quaternary Glaciations – Extent*
924 *and Chronology (2nd Edition)*, 261-278.
- 925 Howe, J.A. Dove, D., Bradwell, T., Gafeira, J. 2012. Submarine geomorphology and glacial history of
926 the Sea of the Hebrides, UK. *Marine Geology* **315-318**, 64-76.
- 927 Huuse, M., Lykke-Andersen, H., Michelsen, O. 2001. Cenozoic evolution of the eastern Danish North
928 Sea. *Marine Geology* **177**, 232-269.
- 929 Hijma, M.P., Cohen, K.M., Roebroeks, W., Westerhoff, W.E., Busschers, F.S. 2012. Pleistocene Rhine-
930 Thames landscapes: Geological background for hominin occupation of the southern North Sea:
931 *Journal of Quaternary Science* **27**, 17-39.
- 932 Hubbard, A., Bradwell, T., Golledge, N., Hall, A., Patton, H., Sugden, D., Cooper, R. and Stoker, M.
933 2009. Dynamic cycles, ice streams and their impact on the extent, chronology and deglaciation of the
934 British-Irish ice sheet. *Quaternary Science Reviews*, **28**, 758–776.

- 935 Hughes, P.D., Gibbard, P.L., Ehlers, J. 2013. Timing of glaciations during the last glacial cycle;
936 Evaluating the concept of a global "Last Glacial Maximum" (LGM). *Earth Science Reviews*, doi:
937 10.1016/j.earscirev.2013.07.003
- 938 Hughes, A.L.C., Gyllencreutz, R., Lohne, Ø.S., Mangerud, J., Svendsen, J.I. 2016. The last Eurasian ice
939 sheets – a chronological database and time-slice reconstruction, DATED-1. *Boreas* **45**, 1-45.
- 940 Huuse, M., Lykke-Andersen, H., Michelsen, O. 2001. Cenozoic evolution of the eastern Danish North
941 Sea. *Marine Geology* **177**, 232-269.
- 942 Jansen, J.H.F., van Weering, T.C.E., Eisma, D. 1979. Late Quaternary Sedimentation in the North Sea.
943 In: Oele, E., Schuttenhelm, R.T.E., Wiggers, A.J. (eds) The Quaternary history of the North Sea. Acta
944 Univ. Ups. Symposium. Univ. Ups Annum Quintegentesimum Celebrantis, Uppsala 2. 175-187
- 945 Kristensen, T.B., Huuse, M., Piotrowski, J.A., Clausen, O.R. 2007. A morphometric analysis of tunnel
946 valleys in the eastern North Sea based on 3D seismic data. *Journal of Quaternary Science* **22**, 801-
947 815.
- 948 Laban, C. 1995. The Pleistocene glaciations in the Dutch Sector of the North Sea. PhD Thesis,
949 Universiteit van Amsterdam, 200 pp.
- 950 Lee, J.R., Phillips, E., Booth, S.J., Rose, J., Jordan, H.M., Pawley, S.M., Warren, M., Lawley, R.S. 2013.
951 A polyphase glaciectonic model for ice-marginal retreat and terminal moraine development: the
952 Middle Pleistocene British Ice Sheet, northern Norfolk, UK. *Proceedings of the Geologists Association*
953 **124**, 753-777.
- 954 Lee, J.R., Phillips, E., Rose, J., Vaughan-Hirsch, D. 2017. The Middle Pleistocene glacial evolution of
955 northern East Anglia, UK: a dynamic tectonostratigraphic–parasequence approach. *Journal of*
956 *Quaternary Science* **32**, 231-260.
- 957 Lonergan, L., Maidment, S.C.R., Collier, J.S. 2006. Pleistocene subglacial tunnel valleys in the central
958 North Sea basin: 3-D morphology and evolution. *Journal of Quaternary Science* **21**, 891-903.
- 959 Mourgues, R., Cobbold, P.R. 2006. Sandbox experiments on gravitational spreading and gliding in the
960 presence of fluid overpressures. *Journal of Structural Geology* **28**, 887-901.
- 961 Murton, D.K., Murton, J.B. 2012. Middle and Late Pleistocene glacial lakes of lowland Britain and the
962 southern North Sea Basin. *Quaternary International* **260**, 115-142.

- 963 Nieuwland, D.A., Leutscher, J.H., Gast, J. 2000. Wedge equilibrium in fold-and-thrust belts:
964 prediction of out-of-sequence thrusting based on sandbox experiments and natural examples.
965 *Geologie en Mijnbouw* **79**, 81-91.
- 966 Ó Cofaigh, C., Evans, D.J.A., Smith, I.R. 2010. Large-scale reorganization and sedimentation of
967 terrestrial ice streams during late Wisconsinan Laurentide ice sheet deglaciation. *Geological Society
968 of America Bulletin* **122**, 743–756.
- 969 Ottesen, D., Dowdeswell, J.A., Bugge, T. 2014. Morphology, sedimentary infill and depositional
970 environments of the Early Quaternary North Sea Basin (56° to 62°N). *Marine and Petroleum Geology*
971 doi: 10.1016/j.marpetgeo.2014.04.007.
- 972 Pedersen, S.A.S., Boldreel, L.O. 2017. Glaciotectonic deformations in the Jammerbugt and the
973 glaciodynamic development in the eastern North Sea. *Journal of Quaternary Science* **32**, 183-195.
- 974 Phillips, E., Merritt, J. 2008. Evidence for multiphase water-escape during rafting of shelly marine
975 sediments at Clava, Inverness-shire, NE Scotland. *Quaternary Science Reviews* **27**, 988-1011.
- 976 Phillips, E., Lee, J.R., Burke, H. 2008. Progressive proglacial to subglacial deformation and syntectonic
977 sedimentation at the margins of the Mid-Pleistocene British Ice Sheet: evidence from north Norfolk,
978 UK. *Quaternary Science Reviews* **27**, 1848-1871.
- 979 Phillips, E., Finlayson, A., Bradwell, T., Everest, J., Jones, J. 2014. Structural evolution triggers a
980 dynamic reduction in active glacier length during rapid retreat: evidence from Falljökull, SE Iceland.
981 *Journal of Geophysical Research: Earth Surface* **119**, doi:10.1002/2014JF003165.
- 982 Phillips, E., Hodgson, D.M., Emery, A.R. 2017. The Quaternary geology of the North Sea Basin.
983 *Journal of Quaternary Geology* **32**, 117-126.
- 984 Phillips, E., Evans, D.J.A., Atkinson, N., Kendall, A. 2017. Structural architecture and glaciectonic
985 evolution of the Mud Buttes cupola hill complex, southern Alberta, Canada. *Quaternary Science
986 Reviews*.
- 987 Ruszczynska-Szenajch, H. 1987. The origin of glacial rafts: Detachment, transport, deposition. *Boreas*
988 **16**, 101-112.
- 989 Ruszczynska-Szenajch, H. 1988. Glaciotectonics and its relationship to other glaciogenic processes. In
990 Croot, D.G. (ed.): *Glaciotectonic Forms and Processes*, 191–193. Balkema, Rotterdam.

- 991 Sejrup, H.P., Aarseth, I., Ellingsen, K.L., Reither, E., Jansen, E., Løvlie, R., Bent, A., Brigham-Grette, J.,
992 Larsen, E., Stoker, M. 1987. Quaternary stratigraphy of the Fladen area, central North Sea: a
993 multidisciplinary study. *Journal of Quaternary Science* **2**, 35-58.
- 994 Sejrup, H.P., Aarseth, I., Hafliðason, H., Løvlie, R., Bratten, Å., Tjøstheim, G., Forsberg, C.F., Ellingsen,
995 K.L. 1995. Quaternary of the Norwegian Channel: glaciation history and palaeoceanography.
996 *Norwegian Journal of Geology* **75**, 65-87.
- 997 Sejrup, H.P., Larsen, E., Landvik, J., King, E.L., Hafliðason, H., Nesje, A., 2000. Quaternary glaciations
998 in southern Fennoscandia: evidence from southwestern Norway and the northern North Sea region,
999 *Quaternary Science Reviews* **19**, 667-685.
- 1000 Sejrup, H.P., Larsen, E., Hafliðason, H., Berstad, I.M., Hjelstuen, B.O., Jonsdottir, H., King, E.L.,
1001 Landvik, J.Y., Longva, O., Nygård, A., Ottesen, D., Raunholm, S., Rise, L., Stalsberg, K. 2003.
1002 Configuration, history and impact of the Norwegian Channel Ice Stream. *Boreas* **32**, 18-36.
- 1003 Sejrup, H.P., Nygard, A., Hall, A.M., Hafliðason, H. 2009. Middle and late Weichselian (Devensian)
1004 glaciation history of south-western Norway, North Sea and eastern UK. *Quaternary Science Reviews*
1005 **28**, 370-380.
- 1006 Sejrup, H.P., Clark, C.D. and Hjelstuen, B.O. 2016. Rapid ice sheet retreat triggered by ice stream
1007 debulking: Evidence from the North Sea. *Geology* **44**, 355–358.
- 1008 Stewart, M.A., Lonergan, L., Hampson, G.J., 2013. 3D seismic analysis of buried tunnel valleys in the
1009 central North Sea: morphology, cross-cutting generations and glacial history. *Quaternary Science*
1010 *Reviews* **72**, 1-17.
- 1011 Stewart, M.A., Lonergan, L., 2011. Seven glacial cycles in the middle-late Pleistocene of northwest
1012 Europe; geomorphic evidence from buried tunnel valleys. *Geology* **39**, 283-286.
- 1013 Stoker, M.S., Balson, P.S., Long, D., Tappin, D.R. 2011. An overview of the lithostratigraphical
1014 framework for the Quaternary deposits on the United Kingdom continental shelf. *British Geological*
1015 *Survey Research Report RR/11/03*. 48 pp.
- 1016 Stride, A.H. 1959. On the Origin of the Dogger Bank, in the North Sea. *Geological Magazine* **96**, 33-
1017 44.
- 1018 Valentin, H. 1955. Die Grenze der letzten Vereisung im Nordseeraum. *Verhandl. Deut. Geografentag*,
1019 *Hamburg* **30**, 359-366.

- 1020 van der Meer, J.J.M., Laban, C., 1990. Micromorphology of some North Sea till samples, a pilot study.
1021 *Journal of Quaternary Science* 5, 95–101.
- 1022 van Gijssel, K. 1987. A lithostratigraphic and glaciotectionic reconstruction of the Lamstedt Moraine,
1023 Lower Saxony (FRG). In van der Meer, J.J.M. (Ed.): *Tills and Glacitectionics*, 145-156, A.A. Balkema,
1024 Rotterdam.
- 1025 Vaughan-Hirsch, D., Phillips, E. 2017. Mid-Pleistocene thin-skinned glaciotectionic thrusting of the
1026 Aberdeen Ground Formation, Central Graben region, central North Sea. *Journal of Quaternary*
1027 *Science* 32, 196-212.
- 1028 Veenstra, H.J. 1965. Geology of the Dogger Bank area, North Sea. *Marine Geology* 3, 245-262.
- 1029 Zanella, E., Coward, M.P. 2003. Structural framework. In: Evans, D., Graham, C., Atmour, A.,
1030 Bathurst, P. (eds) *The Millennium Atlas: Petroleum Geology of the Central and Northern North Sea*.
1031 The Geological Society of London, London. 45–59.

1032

1033 **11. Figures**

1034 **Figure 1. (a)** Map showing the location of the Dogger Bank in the southern North Sea Basin, and the
1035 Round 3 windfarm zone indicated by the red polygon. The limit of the UK territorial waters is also
1036 marked in red. EMODNET DigBath bathymetry (UK waters) and GEBCO bathymetry (Non UK waters);
1037 and **(b)** Map showing the location of the Dogger Bank windfarm zone (DBZ) and Tranches A, B and C,
1038 as well as the extent of the regional and high-resolution seismic surveys acquired during the site
1039 survey.

1040 **Figure 2. (a)** Horizon map constructed for the top of the Older Dogger Bank within Tranche A; and
1041 **(b)** Landform map of the buried glacial landscape concealed within the Dogger Bank Formation
1042 comprising a suite of topographically higher arcuate moraine ridges separated by lower lying basinal
1043 areas and meltwater channels (after Cotterill *et al.*, 2017b).

1044 **Figure 3.** Structural interpretation of lines 1 to 4 from Area A located within the central part of the
1045 thrust-moraine complex (see Figure 2): **(a)** line 1; **(b)** line 2; **(c)** line 3; and **(d)** line 4. A high-
1046 resolution, large format version of this figure is provided as a supplementary publication.

1047 **Figure 4.** Structural interpretation of lines 5 to 8 from Area B located towards the north-western end
1048 of the thrust-moraine complex (see Figure 2): **(a)** line 5; **(b)** line 6; **(c)** line 7; and **(d)** line 8. A high-
1049 resolution, large format version of this figure is provided as a supplementary publication.

1050 **Figure 5.** Structural interpretation of lines 9 to 11 from Area C located towards the south-eastern
1051 end of the thrust-moraine complex (see Figure 2): **(a)** line 9; **(b)** line 10; and **(c)** line 11. A high-
1052 resolution, large format version of this figure is provided as a supplementary publication.

1053 **Figure 6.** Structural interpretation of lines 12 to 15 from Area D (see Figure 2): **(a)** line 12; **(b)** line 13;
1054 **(c)** line 14; and **(d)** line 15. A high-resolution, large format version of this figure is provided as a
1055 supplementary publication.

1056 **Figure 7.** Diagram showing the seismic data (b and d) and detailed structural interpretation (c and e)
1057 of the south-western end of line 3. Line 3 is representative of the glacitectonic deformation
1058 observed within Area A (see Figure 2). The intensity of glacitectonic deformation (folding and
1059 thrusting) increases towards the NE and is largely confined to the seismically brighter Basal Dogger
1060 Bank with the overlying bedded sediments of the Upper Dogger Bank being relatively undeformed
1061 (see text for details).

1062 **Figure 8.** Diagram showing the seismic data (b and d) and detailed structural interpretation (c and e)
1063 of the central part of line 3. Line 3 is representative of the glacitectonic deformation observed within
1064 Area A (see Figure 2). Glacitectonic deformation within this part of the thrust-moraine is dominated
1065 by locally intense SE-directed folding and thrusting of the Basal and Lower Dogger Bank units (see
1066 text for details). The base of the deformed Dogger Bank Formation sequence is marked by a laterally
1067 extensive *décollement* surface.

1068 **Figure 9.** Diagram showing the seismic data (b, d and f) and detailed structural interpretation (c, e
1069 and g) of the north-eastern of line 3. Line 3 is representative of the glacitectonic deformation
1070 observed within Area A (see Figure 2). Glacitectonic deformation within this part of the thrust-
1071 moraine is dominated by locally intense SE-directed folding and thrusting of the Basal and Lower
1072 Dogger Bank units (see text for details). A prominent ridge marking the northern limit of the main
1073 part of thrust-moraine is separated from the remainder of the complex by a c. 1.5 km wide linear
1074 trough or channel filled with variably deformed Upper Dogger Bank sediments.

1075 **Figure 10.** Diagram showing the seismic data (b, d and f) and detailed structural interpretation (c, e
1076 and g) for key parts of line 7. Line 7 is representative of the glacitectonic deformation observed
1077 within Area B (see Figure 2). Glacitectonic deformation within this part of the thrust-moraine is
1078 dominated by locally intense SE-directed folding and thrusting of the Basal and Lower Dogger Bank
1079 units. This deformed sequence is overlain by a locally thick sequence of undeformed Upper Dogger
1080 Bank sediments which also infill deeply incised channels which locally cut through the entire

1081 thickness of the deformed Lower and Basal Dogger Bank units and into the underlying Pre-Dogger
1082 Bank sequence (see text for details).

1083 **Figure 11.** Diagram showing the seismic data (b, d and f) and detailed structural interpretation (c, e
1084 and g) for key parts of line 12. Line 12 is representative of the glacitectonic deformation observed
1085 within Area D (see Figure 2). The moraine ridges are composed of highly deformed (SE-directed
1086 folding and thrusting) Basal and Lower Dogger Bank sediments. The topographic highs formed by the
1087 main moraine complexes identified in the southern and northern parts of the study area are
1088 separated by a low-lying basin filled by typically undeformed Upper Dogger Bank sediments.
1089 However SE-directed deformation associated with the development of the northern moraines can
1090 be seen to propagate upwards from the Basal and Lower Dogger Bank units to affect the overlying
1091 Upper Dogger Bank sediments (see text for details).

1092 **Figure 12.** Diagram showing the proposed conceptual model for the evolution of the main thrust-
1093 moraine complex identified within the southern part of Tranche A in response to the active retreat
1094 of an oscillating ice margin. This model can be divided into a number of stages: **Stage 1** – initial ice
1095 advance across the Basal Dogger Bank unit; **Stage 2** – ice-marginal to proglacial deformation of the
1096 Basal Dogger Bank and the formation of a forward propagating thrust stack; **Stage 3** – retreat of the
1097 ice margin from its advance limit and contemporaneous deposition of a sequence of outwash
1098 sediments; **Stage 4** – readvance of the glacier resulting in ice-marginal to proglacial thrusting of the
1099 outwash sequence deposited in stage 3 and accretion of these deformed sediments (Lower Dogger
1100 Bank) onto the up-ice side of the evolving thrust moraine complex; **Stage 5** – retreat of the ice
1101 margin from the stage 4 advance limit and contemporaneous deposition of a sequence of outwash
1102 sediments; **Stage 6** – further readvance of the glacier resulting in ice-marginal to proglacial thrusting
1103 of the outwash sequence deposited in stage 5 and accretion of the thrust and folded blocks
1104 (Lower Dogger Bank) onto the up-ice side of the thrust moraine complex; **Stage 7** – retreat of the ice
1105 margin from the stage 6 advance limit and contemporaneous deposition of a sequence of outwash
1106 sediments; **Stage 8** – a further readvance of the glacier leading to further SE-directed folding and
1107 thrusting during the accretion of the outwash sediments deposited during stage 7 onto the up-ice
1108 margin of the increasing structurally complex thrust-moraine. Accretion of these relatively younger
1109 thrust and folded sediments may have accompanied the folding of earlier developed thrusts
1110 within the main part of the thrust-moraine to the south; and **Stage 9** onwards – further phases of ice
1111 margin retreat and advance (see text for details).

1112 **Figure 13.** Cartoon showing the active retreat of an ice sheet northwards across Tranche A of the
1113 Dogger Bank (see text for details).

1114

1115 **12. Tables**

1116 **Table 1.** Summary of the characteristics of the Basal, Lower and Upper Dogger Bank subunits
1117 identified on the seismic profiles examined from Tranche A.

| Seismic subunit | Description |
|-------------------------|---------------------------------------------------------------------------------------------------------------------------------------------------------------------------------------------------------------------------------------------------------------------------------------------------------------------------------------------------------------------------------------------------------------------------------------------------------------------------------------------------------------------------------------------------------|
| Basal Dogger Bank (BDB) | Structurally lowest unit within the Dogger Bank Formation (0-30 m thick); distinguished by its overall brighter appearance on the seismic profiles; upper surface marked by a band of bright reflectors interpreted as a prominent desiccation/weathering surface; varies from acoustically "massive"/"structureless" to containing laterally variably dipping reflectors; reflectors locally appear crenulated/folded and/or disrupted due to glacitectonic deformation; base interpreted as a laterally extensive décollement surface |
| Lower Dogger Bank (LDB) | Represents main deformed part of Dogger Bank Formation (up to 40-50 m thick); acoustic appearance highly variable ranging from acoustically "blank", lacking internal reflectors and apparently internally "massive"/"structureless", through to stratified, containing weakly to strongly developed reflectors; laterally variably dipping reflectors; reflectors locally appear folded and/or disrupted due to glacitectonic deformation; upper surface locally marked by a band of bright reflectors interpreted as a desiccation/weathering surface |
| Upper Dogger Bank (UDB) | Structurally highest unit within the Dogger Bank Formation (0-50 m thick); acoustic character is laterally variable ranging from areas with no ("blank") or very weakly developed reflectors through to sections with moderately to strongly developed subhorizontal (bedding) to inclined (foresets) reflectors; base of unit irregular (erosive) and clearly truncates structures identified within the underlying subunits |

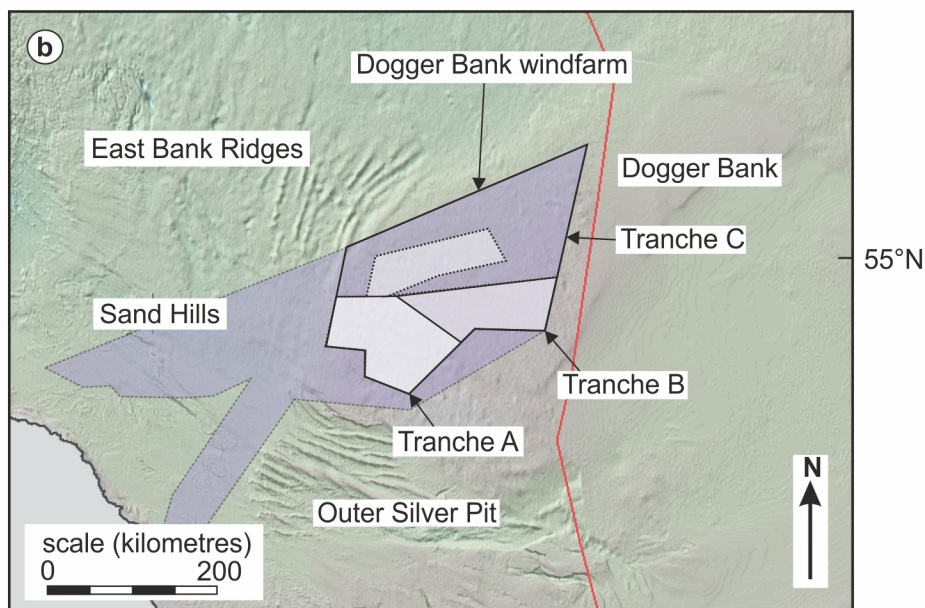
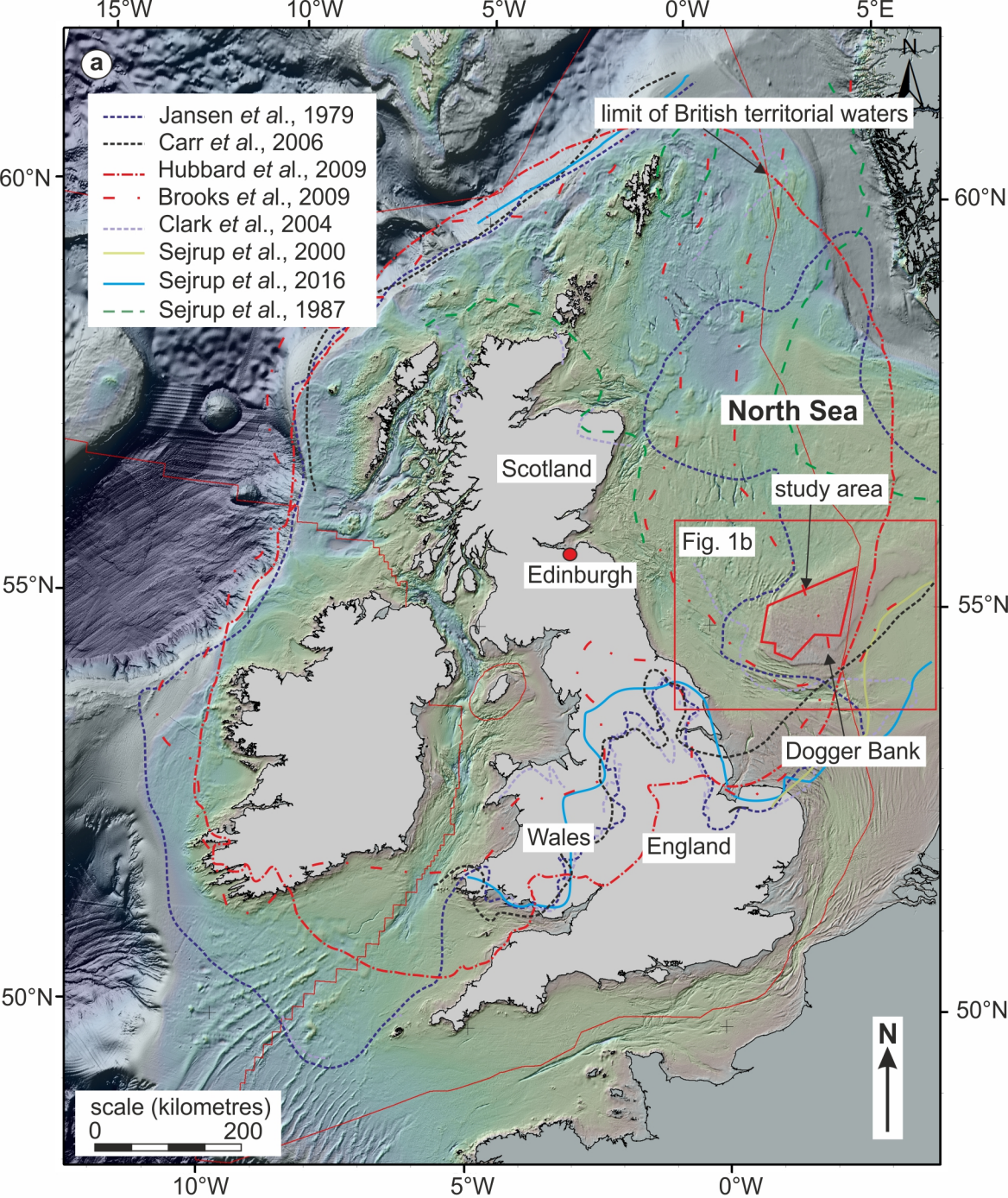
1118

1119

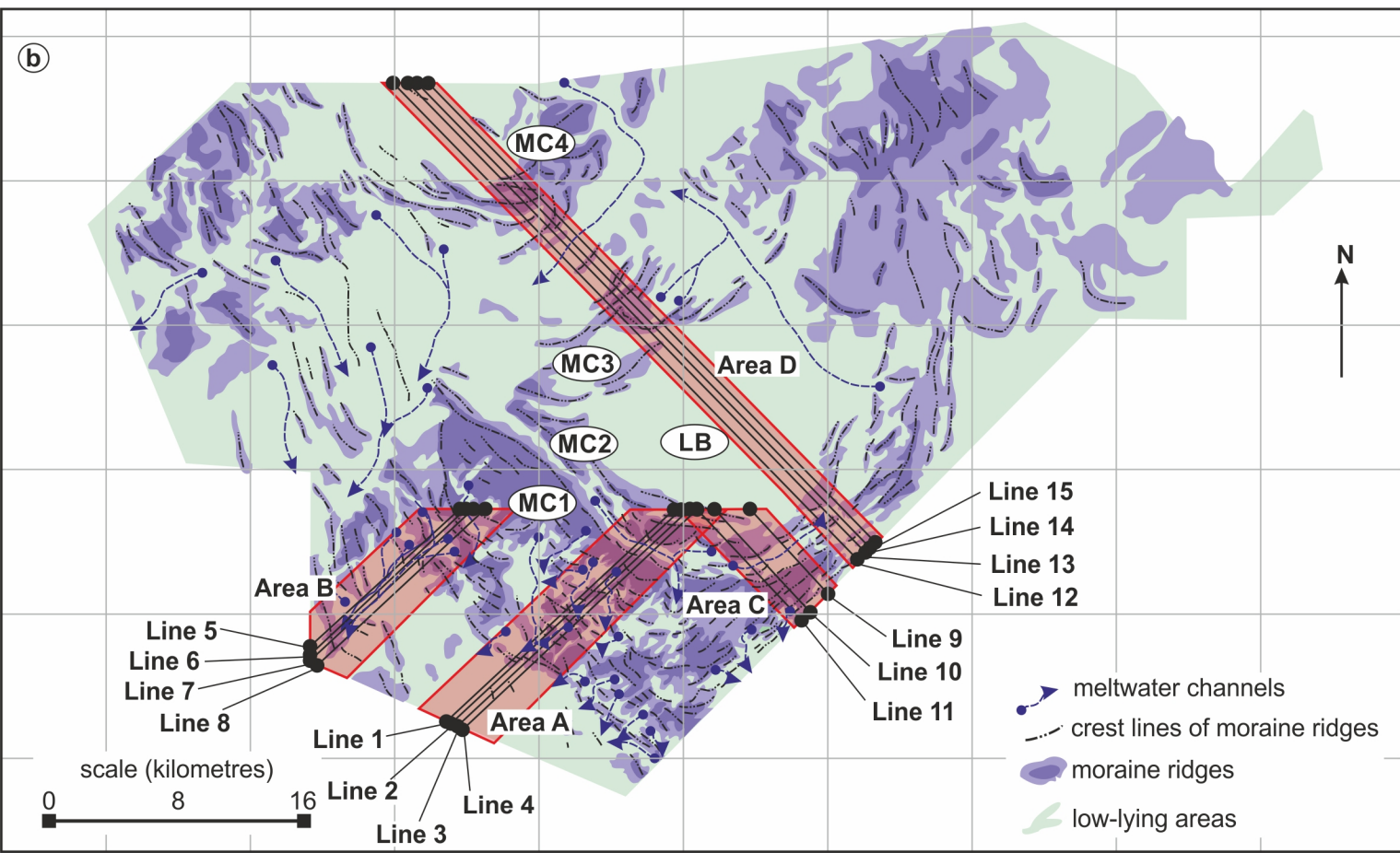
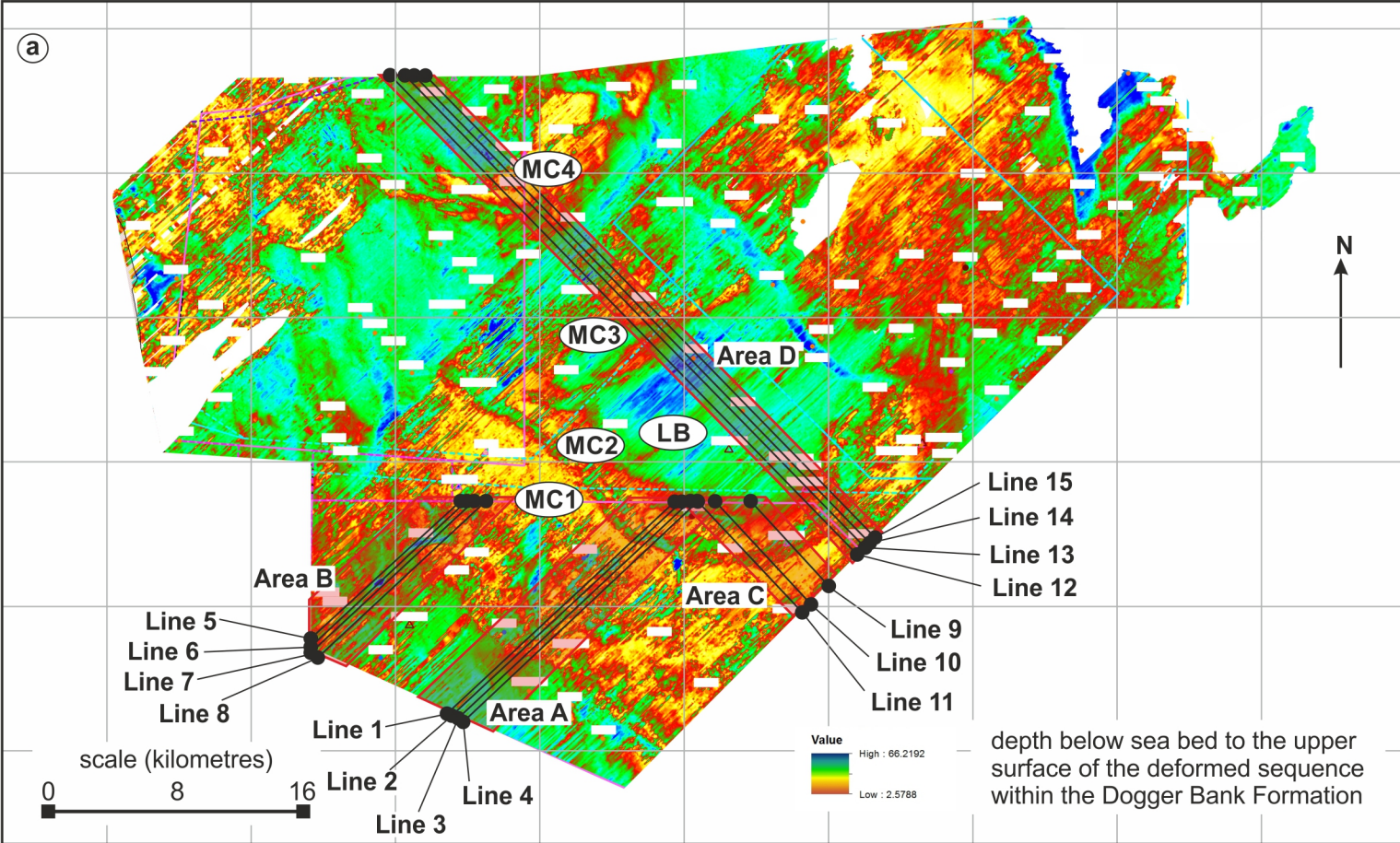
1120 **Table 2.** Summary of the characteristic features of the eight structural domains identified within the
 1121 Dogger Bank Formation of Tranche A (after Cotterill *et al.*, 2017a).

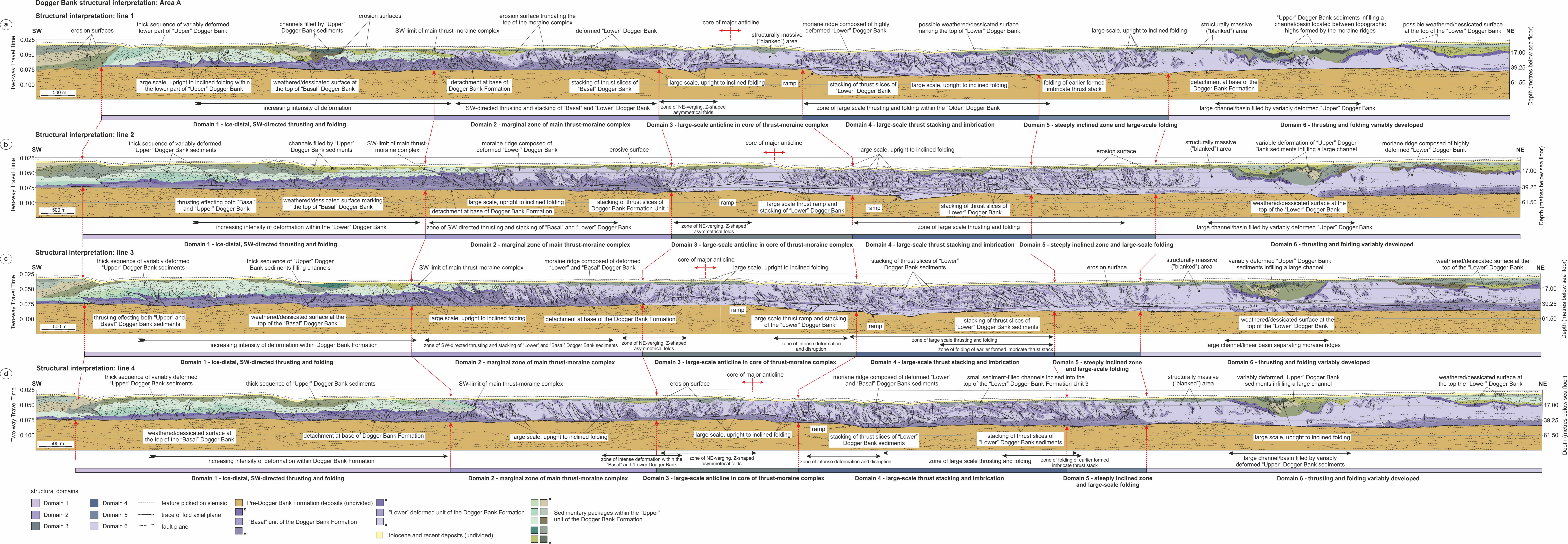
| Domain | Description | Comments |
|--------|----------------------------------------------------------------------------------------------------------------------------------------------------------------------------------------------------------------------------------------------------------------------------------------------|----------------------------------------------------------------------------------------------------------------------------------------------------------------------------------------|
| 1 | Dominated by southerly directed thrusting and folding of both Basal and Upper Dogger Bank sediments, and characterised by the progressive increase in the relative intensity of deformation northwards towards the southern margin of the moraine complex | Interpreted as a forward propagating thrust stack denoting the leading edge of the thrust-moraine complex |
| 2 | Zones of well-developed, S/SE-directed thrusting and folding affecting the Basal and Lower Dogger Bank sediments | |
| 3 | Zones of large-scale (≥ 1 km wavelength), upright folding deforming the Lower Dogger Bank. The presence of these large-scale, warp-like folds is recognised by the change in vergence of parasitic (S, M and Z-shaped), mesoscale folds (50-200 m wavelength) developed on their limbs | Domain 3 is typically developed within the cores of the larger thrust moraine |
| 4 | Dominated by stacked, elongate thrust-bound slices (1-2 km long) of Lower Dogger Bank sediments | |
| 5 | Highly deformed parts of the sequence characterised by steeply inclined reflectors (bedding) and interpreted as denoting zones of relatively intense folding and thrusting | |
| 6 | Most widely developed of the structural domains corresponding to parts of the Lower Dogger Bank where reflectors are either very poorly developed or absent (blanked areas) on the seismic lines | Interpreted as indicating parts of the sequences which are either massive and/or highly disrupted due to deformation |
| 7 | Currently only identified in Area B and corresponds to large (0.5-1 km wide), deeply incised channels filled by a thick sequence of Upper Dogger Bank sediments. | Interpreted as ice-marginal to proglacial meltwater channels cut through the deformed Basal and Lower Dogger Bank units and into the underlying pre-Dogger Bank sequence |
| 8 | Characterised by a thick sequence of typically undeformed Upper Dogger Bank sediments. Horizontal to gently inclined reflections are interpreted as representing primary bedding and large-scale foresets preserved within this sedimentary sequence | Interpreted as a complex sequence of Upper Dogger Bank outwash sediments which infill the larger sedimentary basins formed between the topographic highs formed by the thrust moraines |

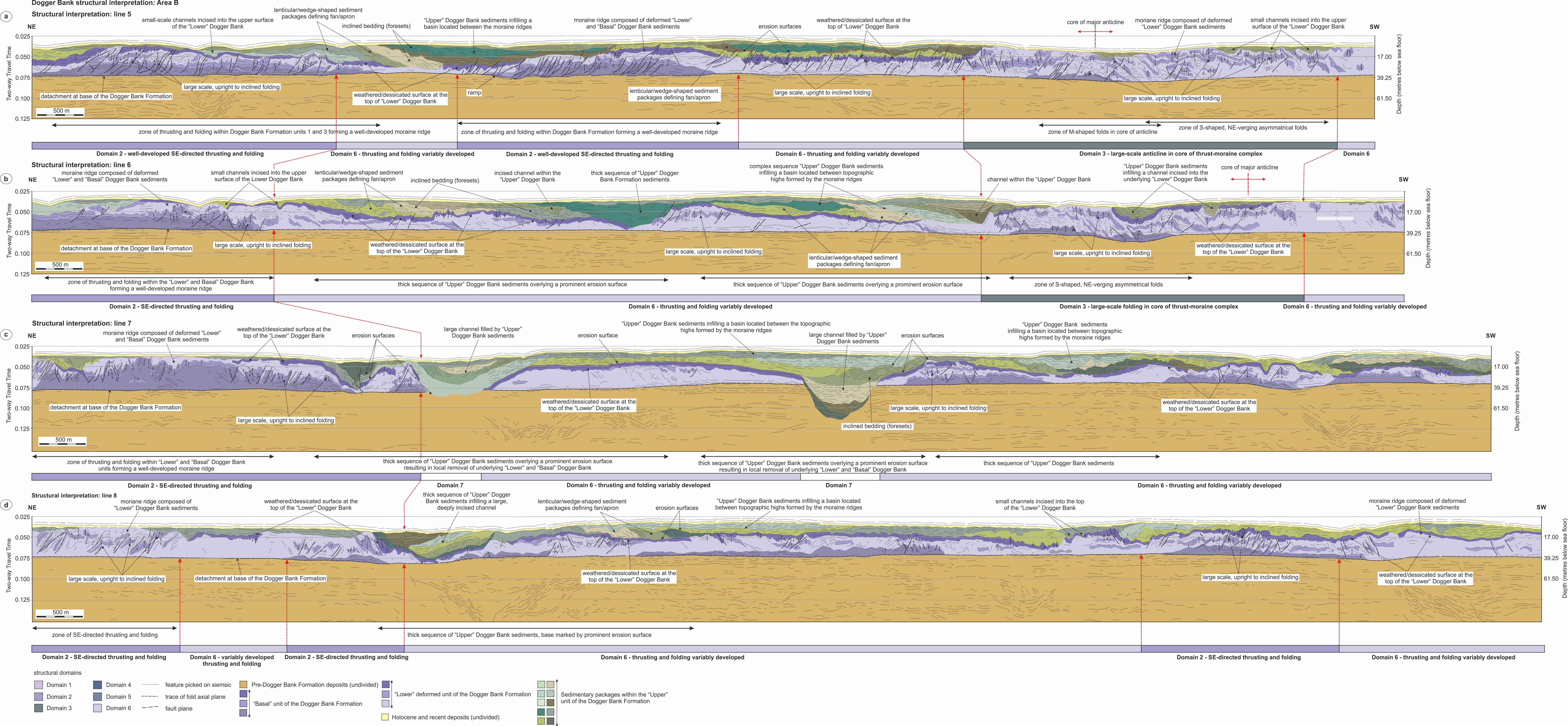
1122

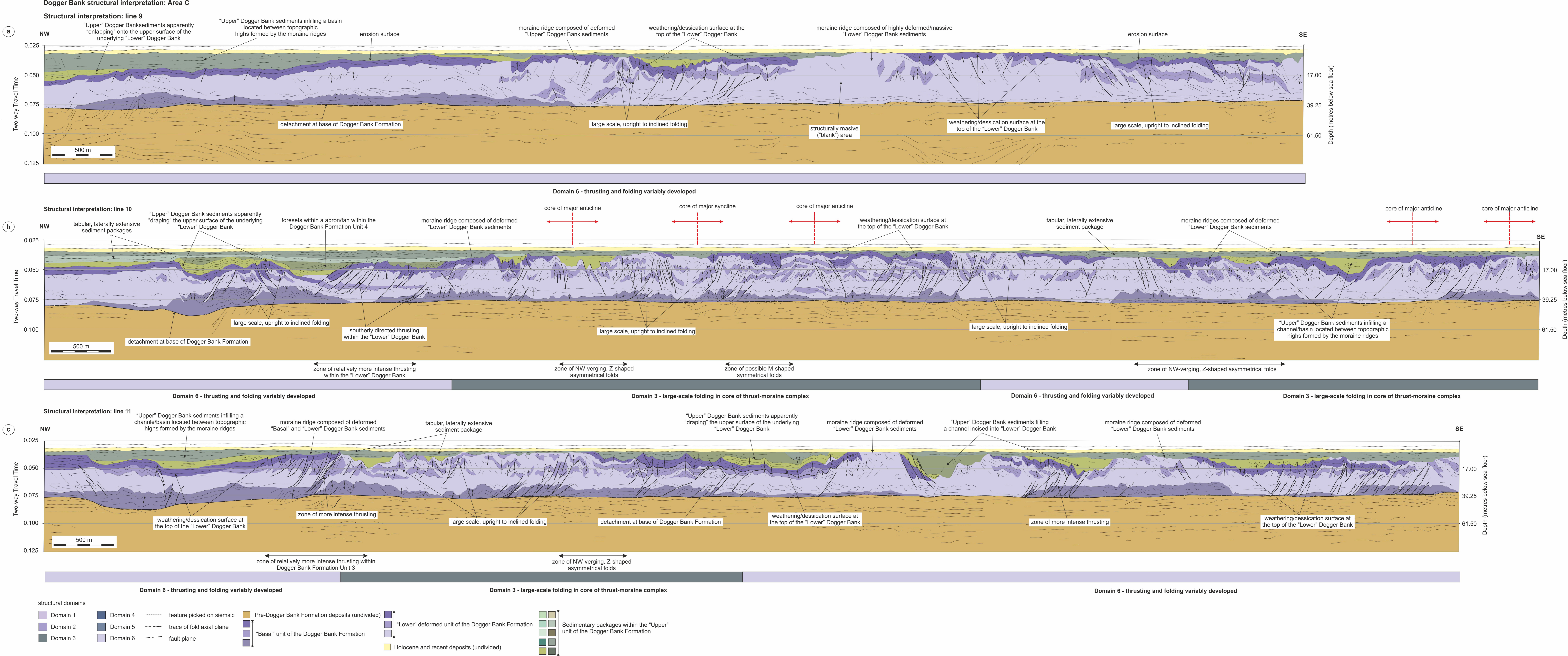


- extent of regional subsurface seismic profiles
 extent of high-resolution subsurface seismic profiles

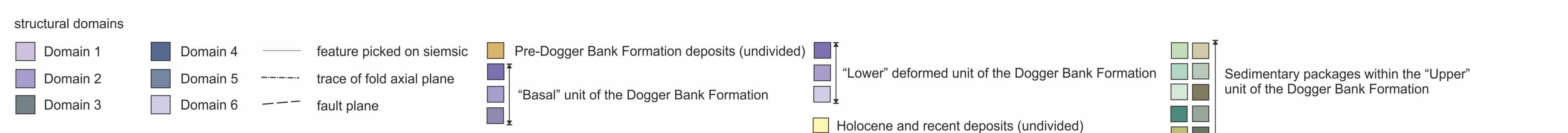
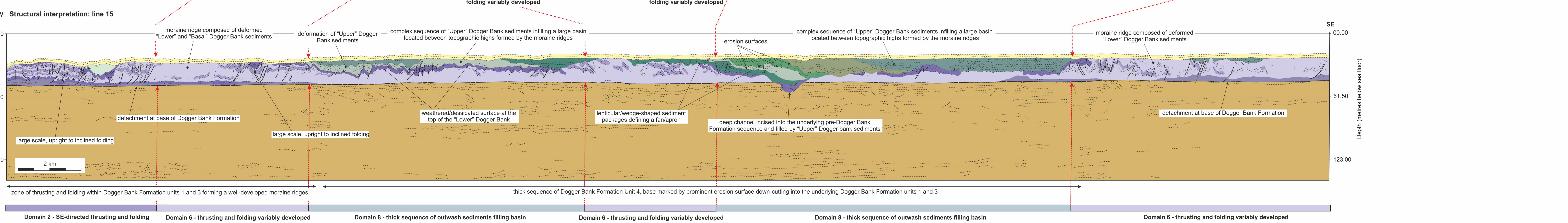
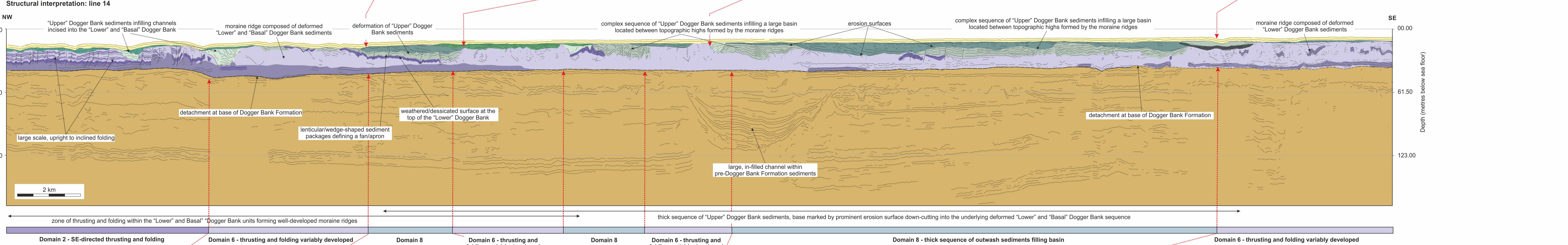
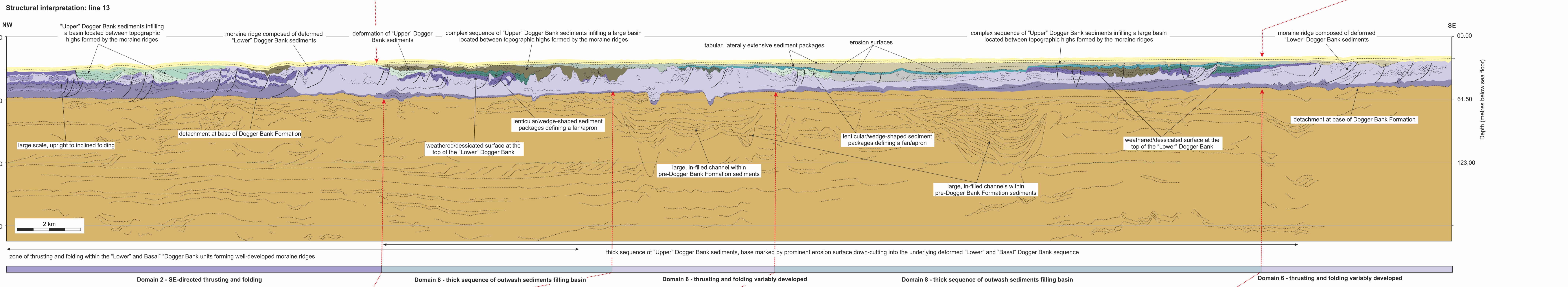
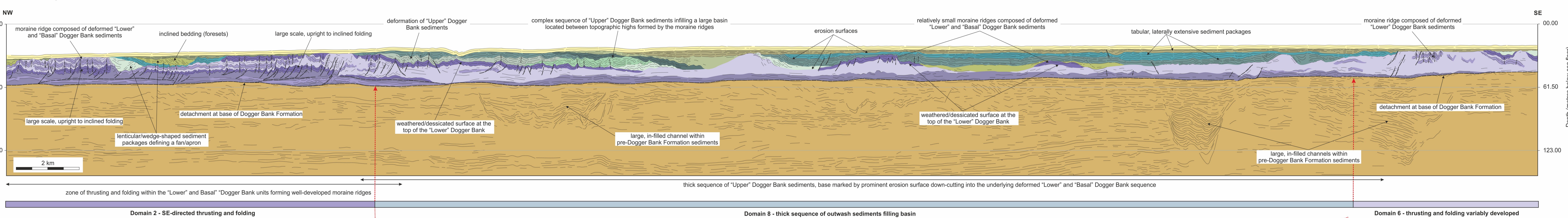




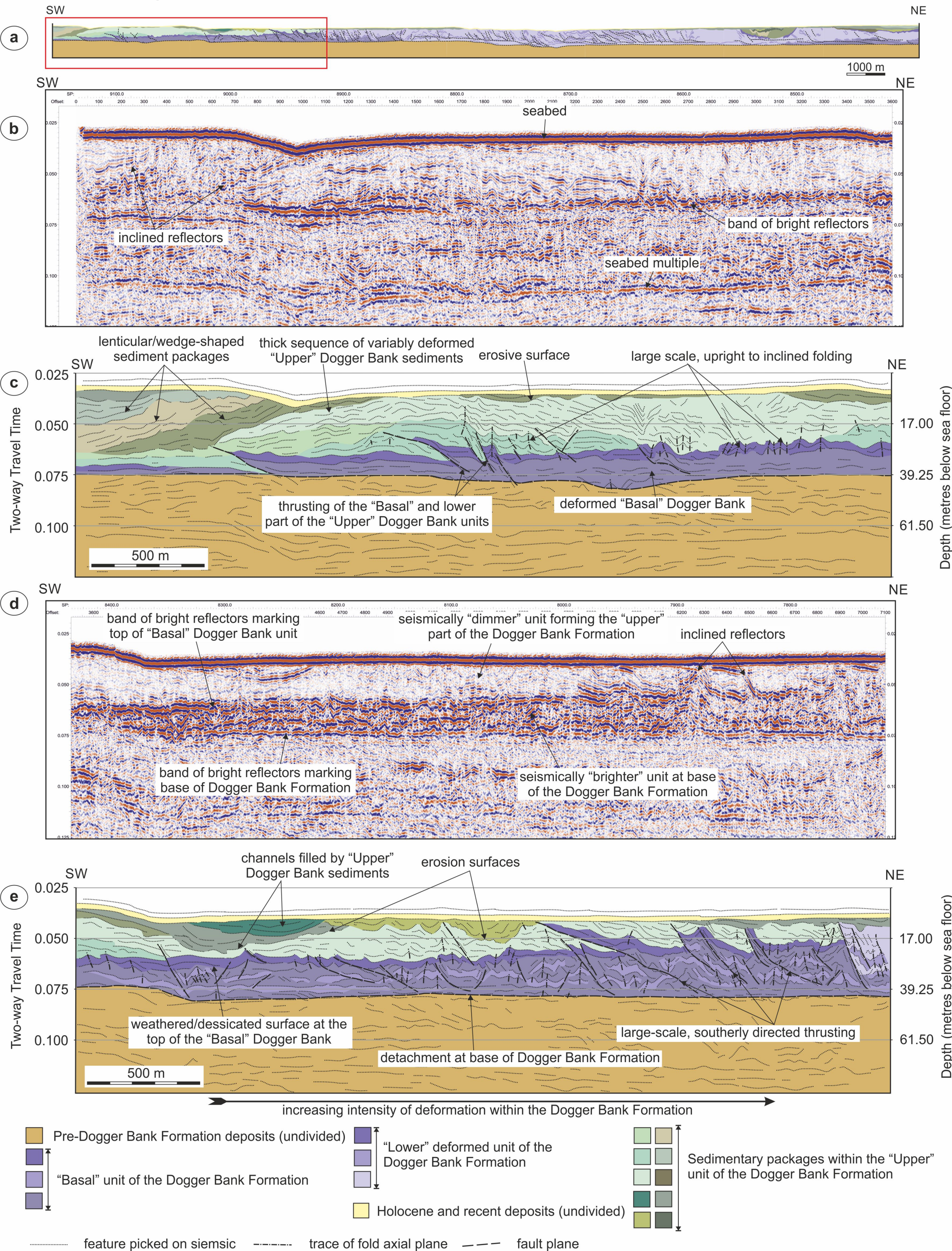




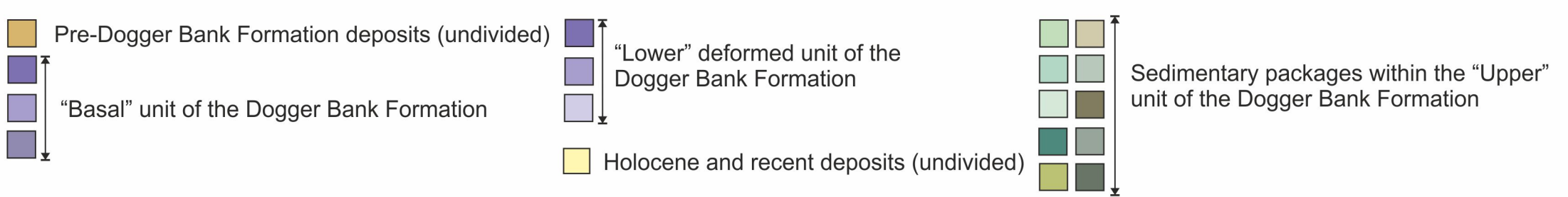
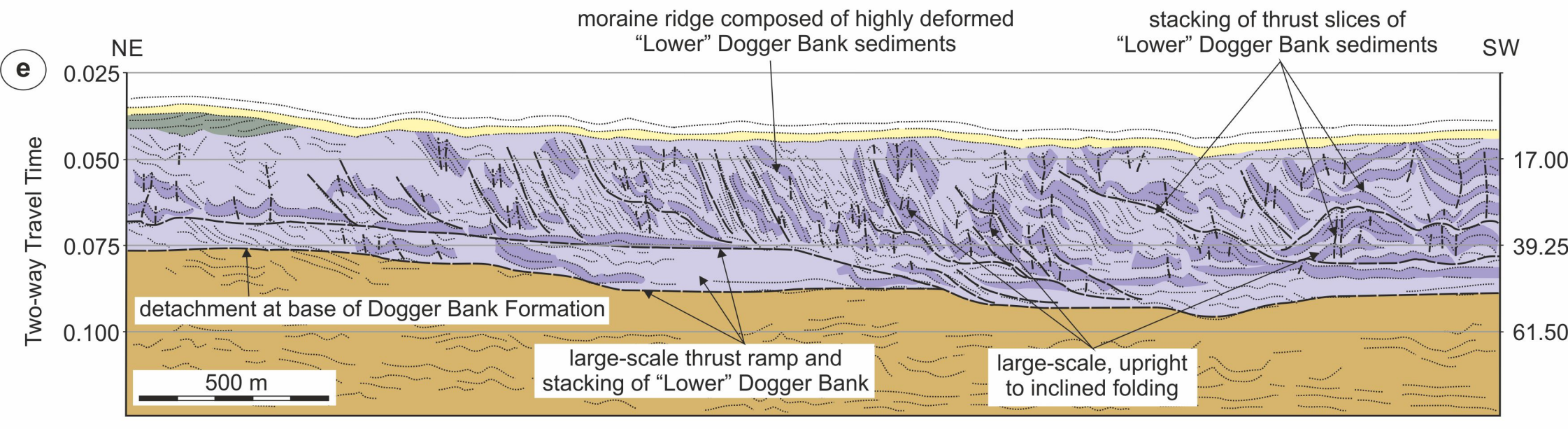
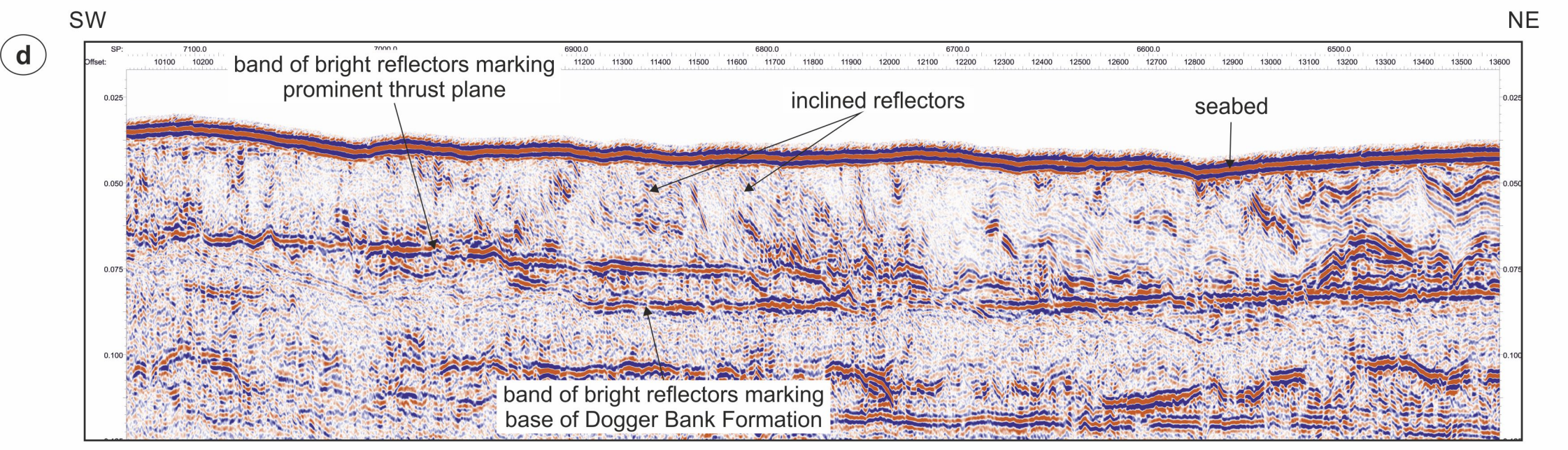
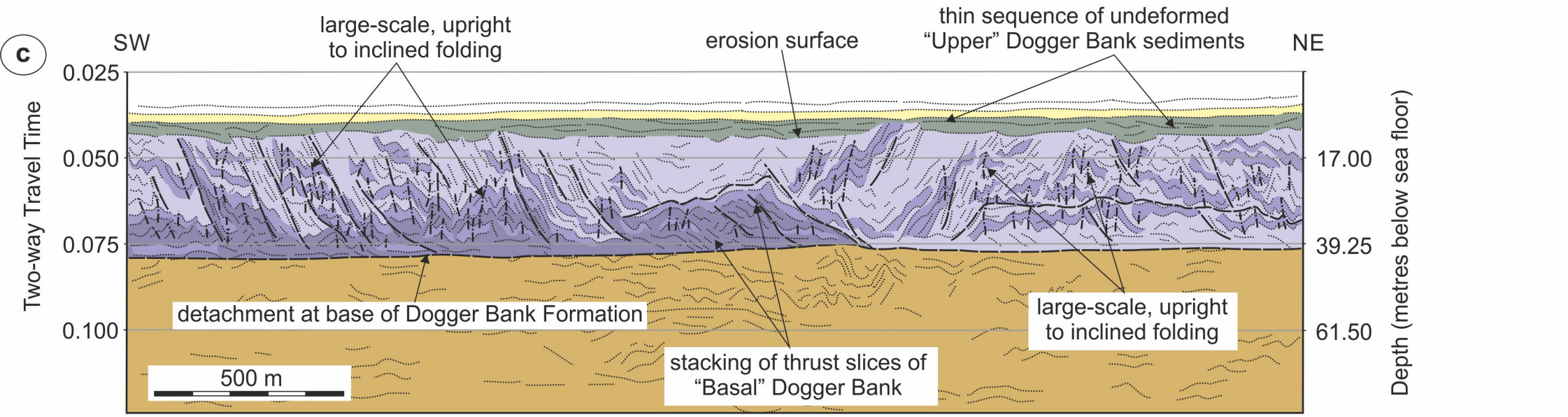
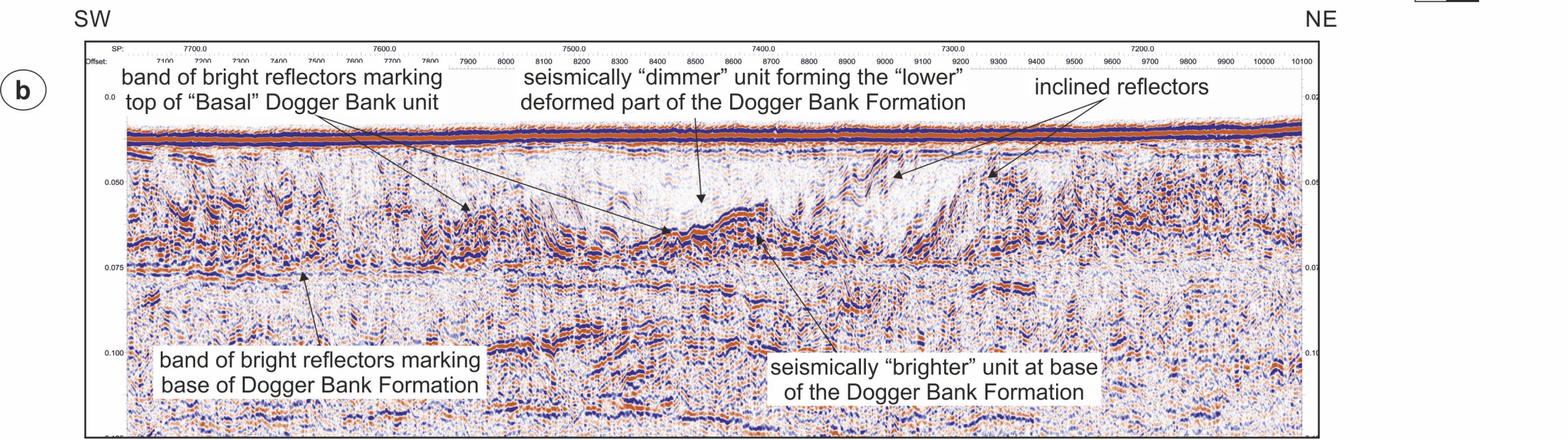
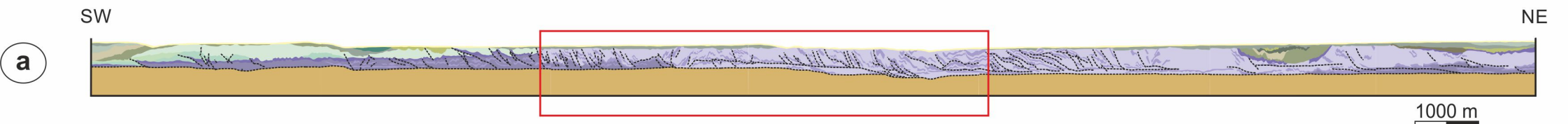
Dogger Bank structural interpretation: Area D



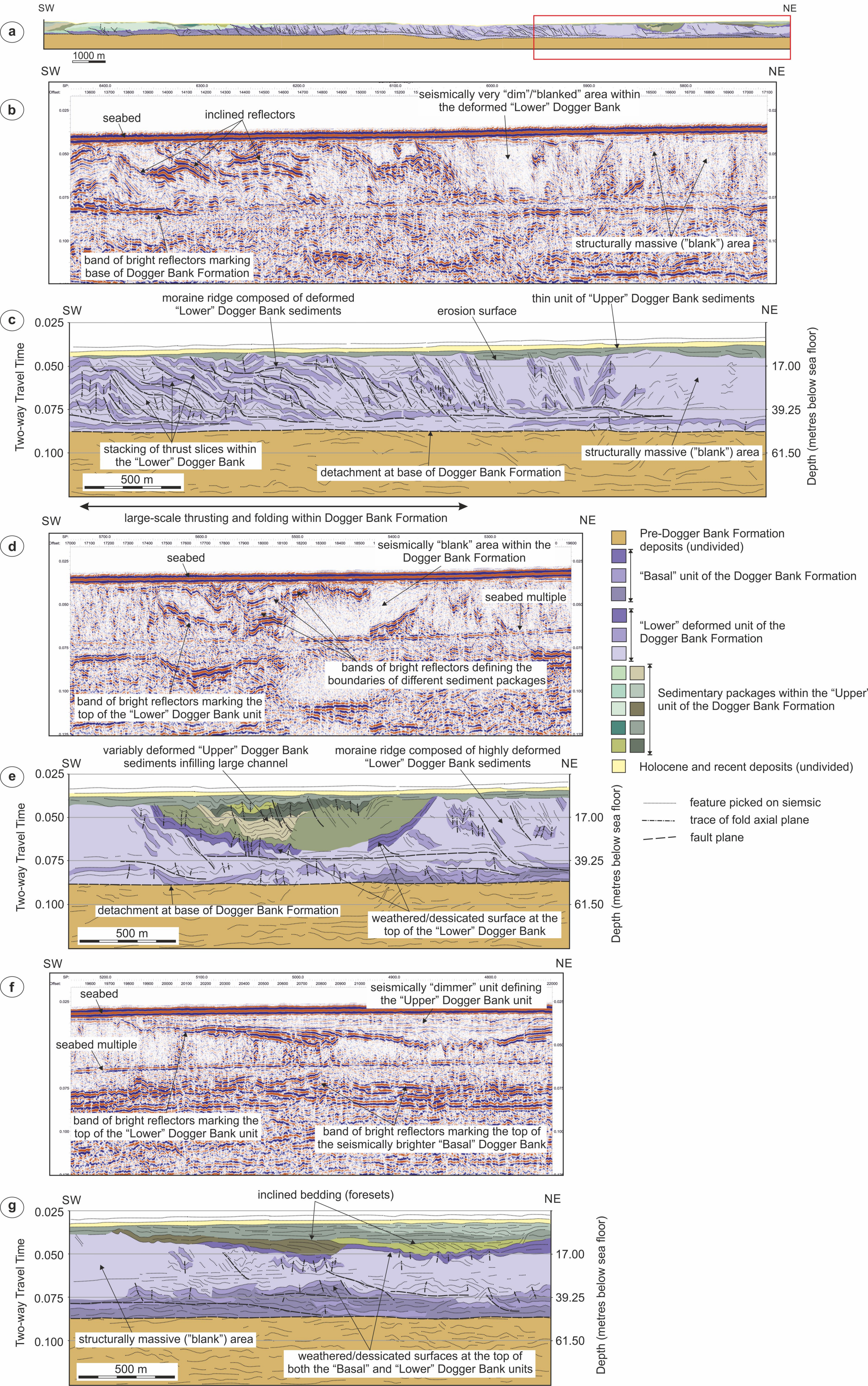
Structural interpretation: line 3



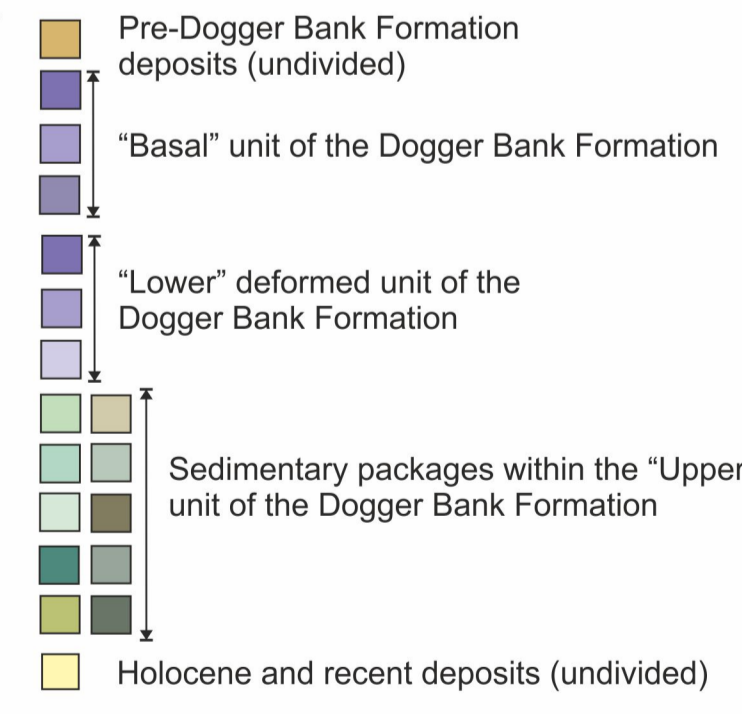
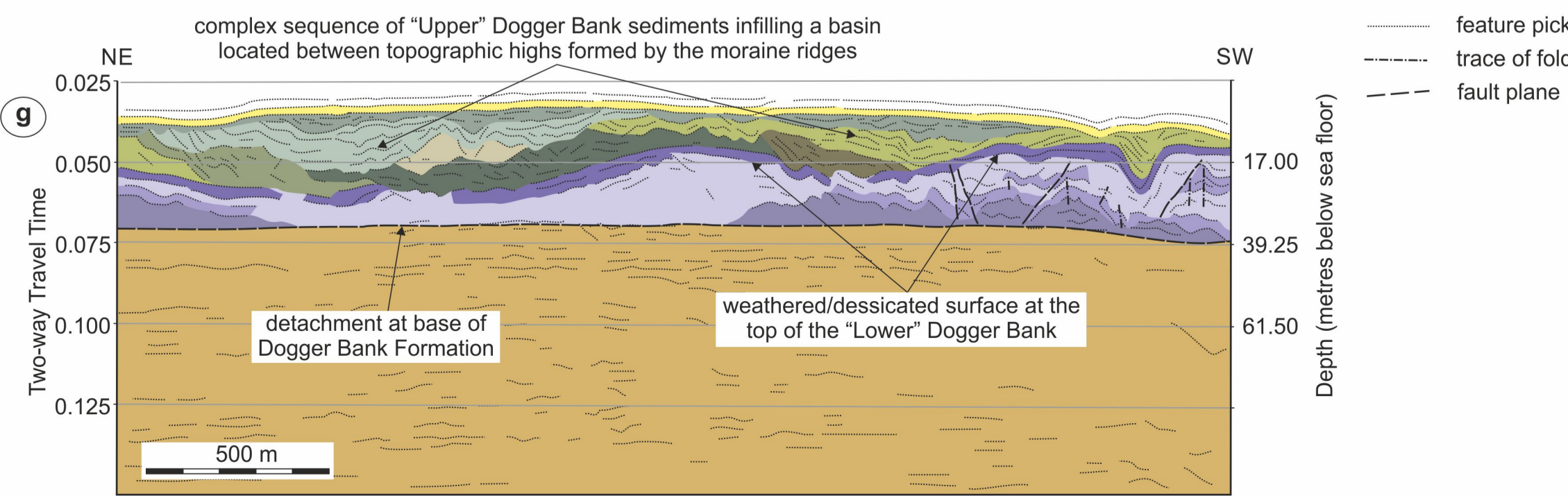
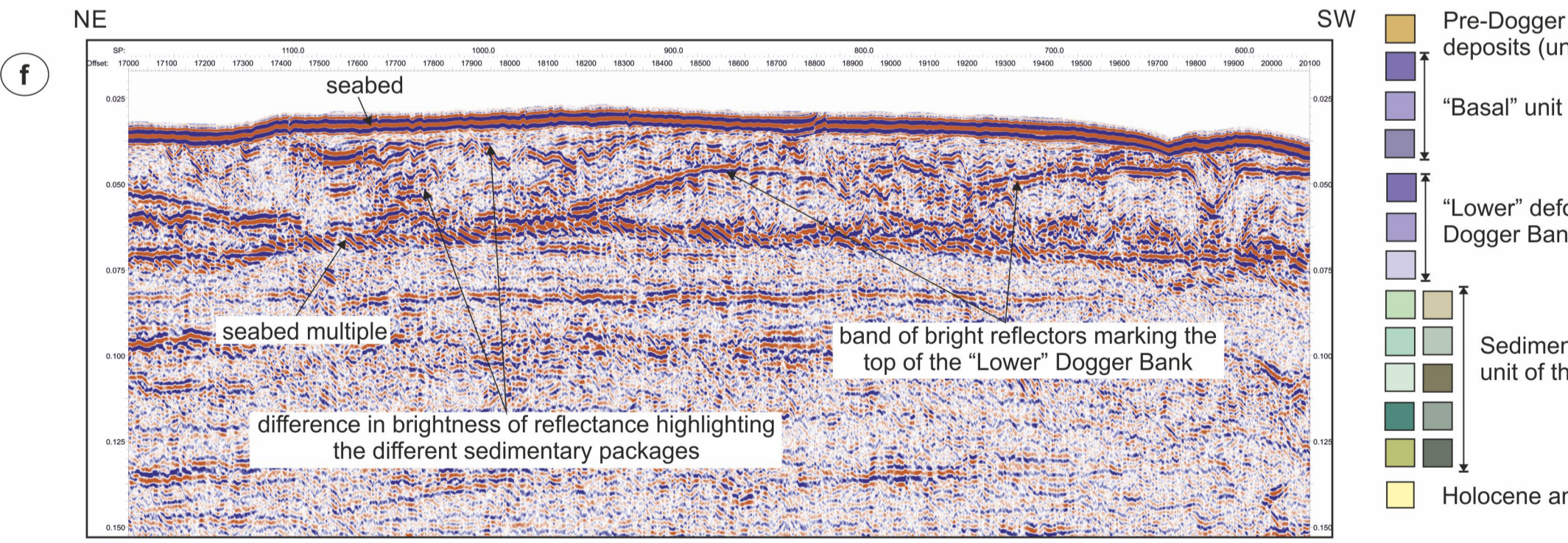
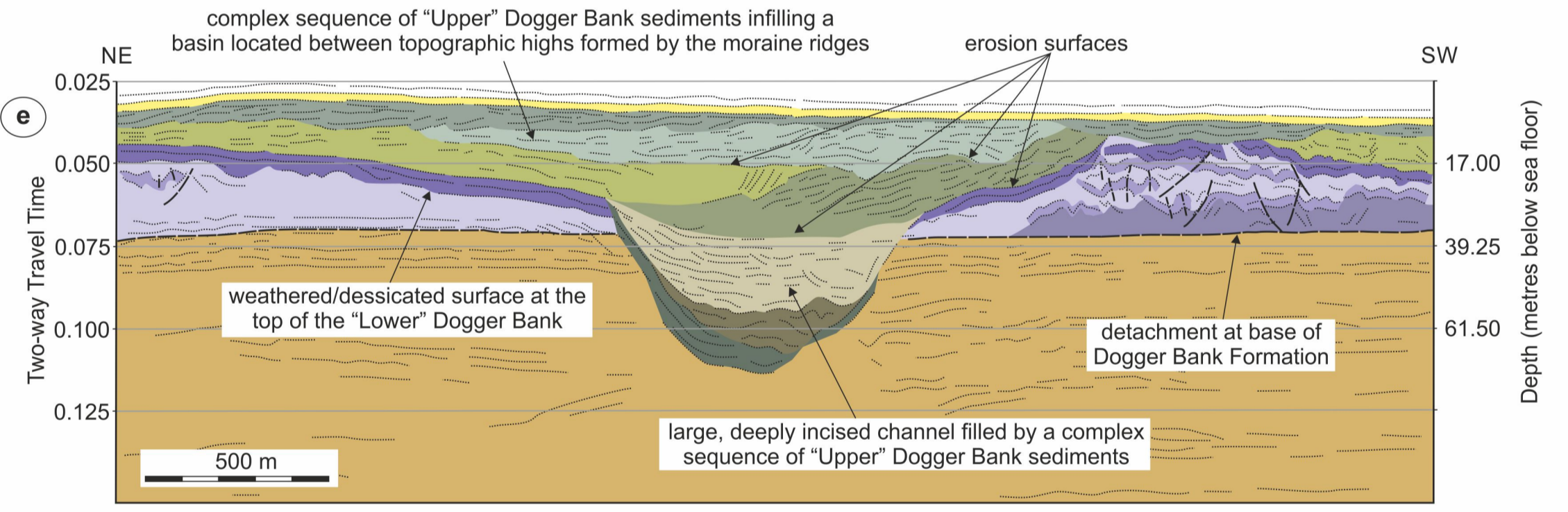
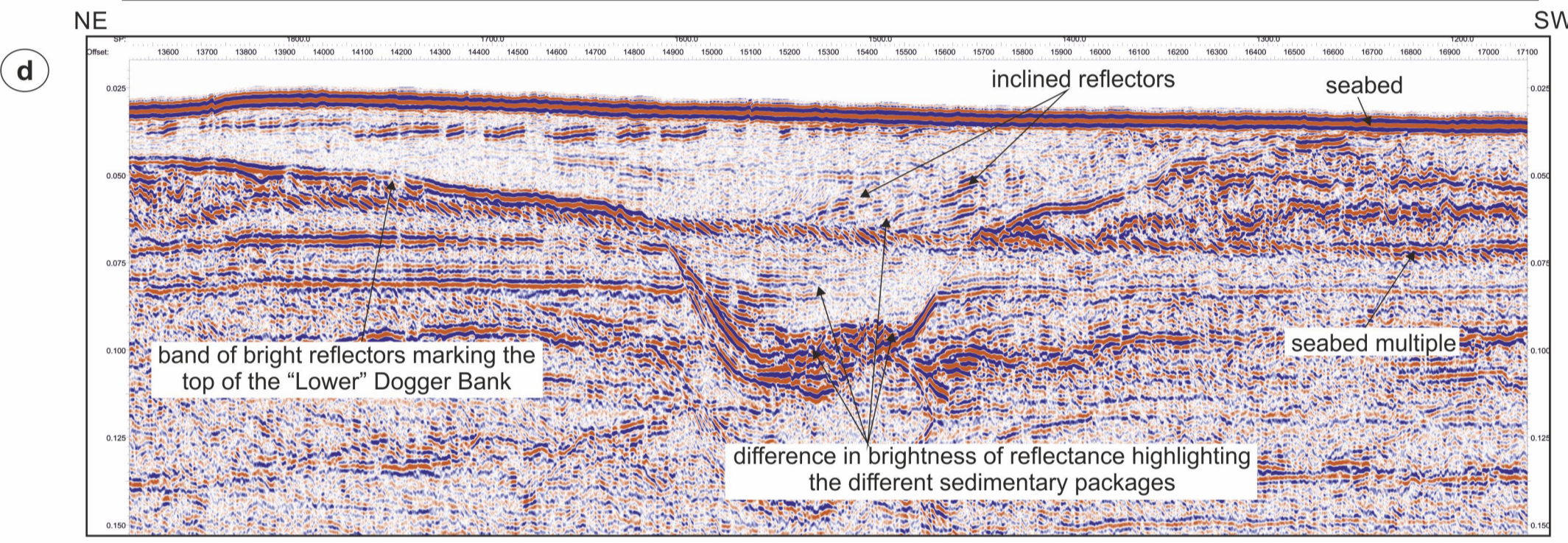
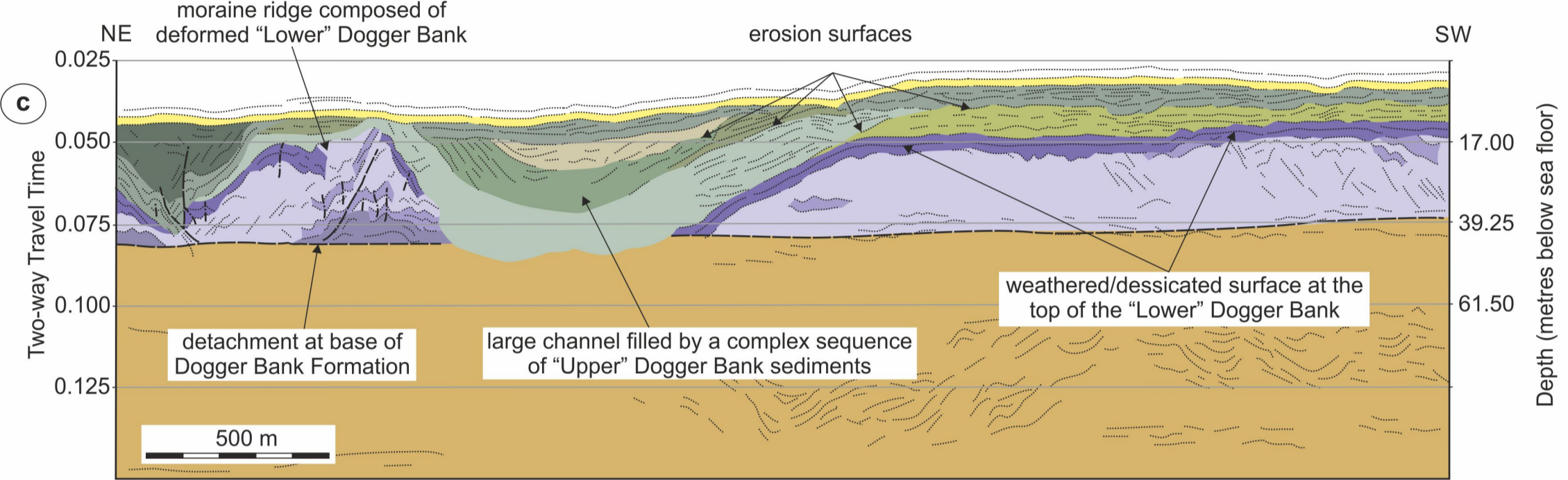
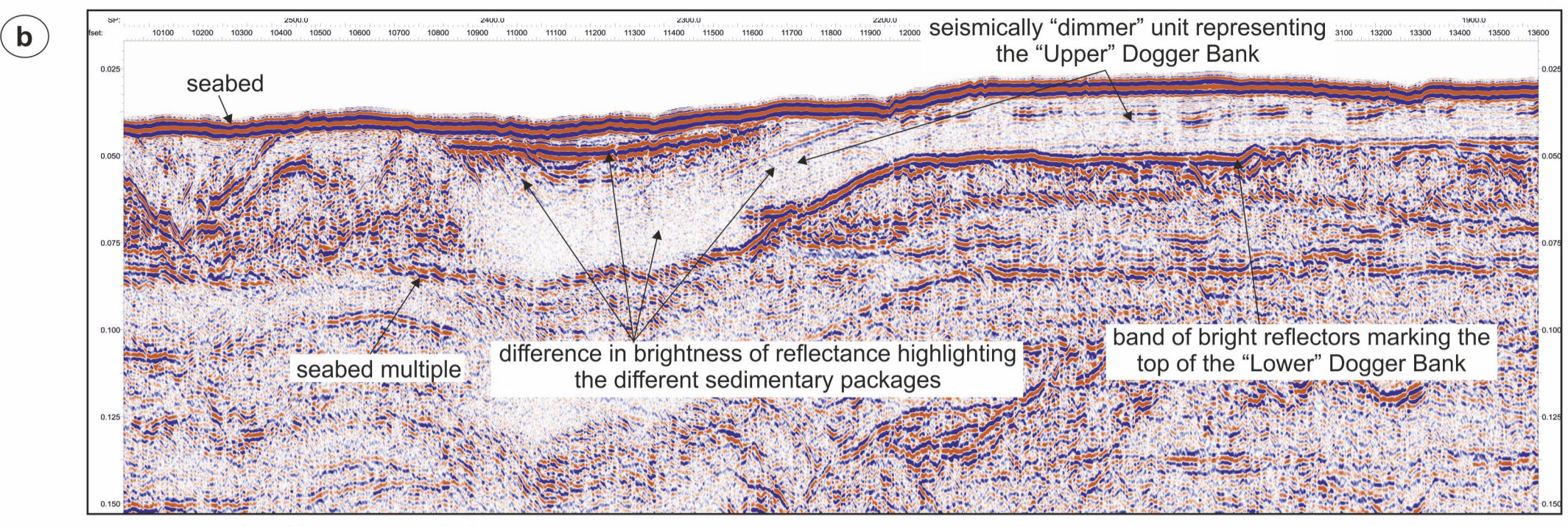
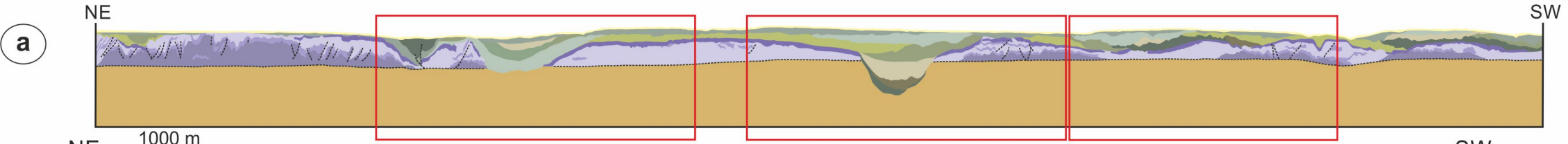
Structural interpretation: line 3



Structural interpretation: line 3



Structural interpretation: line 7



Structural interpretation: line 12

